Supporting Information

Effects of the N-terminal Dynamics on the Conformational States of Human Dopamine Transporter

Liang Xu[*] and Liao Y. Chen

Department of Physics and Astronomy, University of Texas at San Antonio, One UTSA Circle, San Antonio, TX, 78249, USA. *E-mail: liang.xu@utsa.edu; or liang.xu.cc@gmail.com.

Table of Content

```
LeuT   ------------------------------------------------------------ 0
hSERT  METTPLNSQKQLSACEDGEDCQENGVLQKVVPTPGDKVESGQISNGYSAVPSPGAGDDTR 60
dDAT   -------------------------------------------------MSPTGHISK-- 9
hDAT   ---------------MSKSKCSV-GLMSSVVAPAKEPNAVGPKEVELILVKEQNGVQL-- 42


LeuT   --------------MEVKREHWATRLGLILAMAGNAVGLGNFLRFPVQAAENGGGAFMIP 46
hSERT  HSIPATTTTLVAELHQGERETWGKKVDFLLSVIGYAVDLGNVWRFPYICYQNGGGAFLLP 120
dDAT   -SKTPTPHDNDNNSISDERETWSGKVDFLLSVIGFAVDLANVWRFPYLCYKNGGGAFLVP 68
hDAT   -TSSTLTNPRQSPVEAQDRETWGKKIDFLLSVIGFAVDLANVWRFPYLCYKNGGGAFLVP 101
                        .** *. .:.::*:: * **.*.*. ***  . .******::*

LeuT   YIIAFLLVGIPLMWIEWAMGRYGGAQGHGTTPAIFYLLWRNRF--AKILGVFGLWIPLVV 104
hSERT  YTIMAIFGGIPLFYMELALGQYHRNGCISI--------WRKICPIFKGIGYAICIIAFYI 172
dDAT   YGIMLVVGGIPLFYMELALGQHNRKGAITC--------WGRLVPLFKGIGYAVVLIAFYV 120
hDAT   YLLFMVIAGMPLFYMELALGQFNREGAAGV--------WK-ICPILKGVGFTVILISLYV 152
       * :   :.  *:**::* *:*:.         *       * :*     * : :

LeuT   AIYYVYIESWTLGFAIKFLVGLVPEPPPN-------ATDP---DSI-------------- 140
hSERT  ASYYNTIMAWALYYLISSFTDQLPWTSCKNSWNTGNCTNYFSEDNITW------------ 220
dDAT   DFYYNVIIAWSLRFFFASFTNSLPWTSCNNIWNTPNCRPFESQNASRVPVIGNYSDLYAM 180
hDAT   GFFYNVIIAWALHYLFSSFTTELPWIHCNNSWNSPNCSDAHPGDSSGD------------ 200
        :*   * :*:*  ::  :.  :.  :*      :          .        :

LeuT   --------------------------LRPFKEFLYSYIGVP---KGDEPILKPSLFAY 169
hSERT  -----------------------TLHSTSPAEEFYTRHVLQIHRSKGLQDLGGIS-WQL 255
dDAT   GNQSLLYNETYMNGSSLDTSAVGHVEGFQSAASEYFNRYILELNRSEGIHDLGAIK-WDM 239
hDAT   -----------------SSGLNDTFG-TTPAAEYFERGVLHLHQSHGIDDLGPPR-WQL 240
                                *:   :    .*.  :          :

LeuT   IVFLITMFINVSILIRGISKGIERFAKIAMPTLFILAVFLVIRVFL-LETPNGTAADGLN 228
hSERT  ALC---IMLIFTVIYFSIWKGVKTSGKVVWVTATF--PYIILSVLLVRGATLPGAWRGVL 310
dDAT   ALC---LLIVYLICYFSLWKGISTSGKVVWFTALF--PYAVLLILLIRGLTLPGSFLGIQ 294
hDAT   TAC---LVLVIVLLYFSLWKGVKTSGKVVWITATM--PYVVLTALLLRGVTLPGAIDGIR 295
        :.:  :   :  .: **:. .*:. * :   : :: :*       : *:

LeuT   FLWTPDFEKLKDPGVWIAAVGQIFFTLSLGFGAIITYASYVRKDQDIVLSGLTAATLNEK 288
hSERT  FYLKPNWQKLLETGVWIDAAAQIFFSLGPGFGVLLAFASYNKFNNNCYQDALVTSVVNCM 370
dDAT   YYLTPNFSAIYKAEVWVDAATQVFFSLGPGFGVLLAYASYNKYHNNVYKDALLTSFINSA 354
hDAT   AYLSVDFYRLCEASVWIDAATQVCFSLGVGFGVLIAFSSYNKFTNNCYRDAIVTTSINSL 355
        . ::  :.  **: *. *: *:*. ***.:::::** :  ::   ..: :: :*

LeuT   AEVILGGSISIPAAVAFFGV---ANAVAIAKAGAFNLGFITLPAIFSQTAGGTFLGFLWF 345
hSERT  TSFVSGFVI--FTVLGYMAEMRNEDVSEVAKDAGPSLLFITYAEAIANMPASTFFAIIFF 428
dDAT   TSFIAGFVI--FSVLGYMAHTLGVRIEDVAT-EGPGLVFVVYPAAIATMPASTFWALIFF 411
hDAT   TSFSSGFVV--FSFLGYMAQKHSVPIGDVAK-DGPGLIFIIYPEAIATLPLSSAWAVVFF 412
       :.. * :   : :.::.    :*. . .* *:     ::    .: ..::*

LeuT   FLLFFAGLTSSIAIMQPMIAFLEDELKLSR-KHAVLWTAAIVFF--SAHLVMFLNK---S 399
hSERT  LMLITLGLDSTFAGLEGVITAVLDEFPHVWAKRRERFVLAVVITCFFGSLVTLTFGGAYV 488
dDAT   MMLLTLGLDSSFGGSEAIITALSDEFPKIK-RNRELFVAGLFSLYFVVGLASCTQGGFYF 470
hDAT   IMLLTLGIDSAMGGMESVITGLIDEFQLLH-RHRELFTLFIVLATFLLSLFCVTNGGIYV 471
       ::*:  *: *::.  : :*: : **:     :.   :.   :.        *

LeuT   LDEMDFWAGTIGVVFFGLTELIIFFWIFGADKAWEEINRGGIIKVPRIYYYVMRYITPAF 459
hSERT  VKLLEEYATGPAVLTVALIEAVAVSWFYGITQFCRDVKEMLGFSPGWFWRICWVAISPLF 548
dDAT   FHLLDRYAAGYSILVAVFFEAIAVSWIYGTNRFSEDIRDMIGFPPGRYWQVCWRFVAPIF 530
hDAT   FTLLDHFAAGTSILFGVLIEAIGVAWFYGVGQFSDDIQQMTGQRPSLYWRLCWKLVSPCF 531
       .  :: :*   .::   : * *:. *::*   :   ::           :    ::* *

LeuT   LAVLLVVWAREYIPKIMEETHWTVWITR---------FYIIGLFLFLTFLVFLAE----- 505
hSERT  LLFIICSFLMSPPQLRLFQYNYPYWSIILGYCIGTSSFICIPTYIAYRLIITPGTFKERI 608
dDAT   LLFITVYGLIGYEPLTYADYVYPSWANALGWCIAGSSVVMIPAVAIFKLLSTPGSLRQRF 590
hDAT   LLFVVVVSIVTFRPPHYGAYIFPDWANALGWVIATSSMAMVPIYAAYKFCSLPGSFREKL 591
       * .:                 :  *            . :     :    :    .

LeuT   -----RRRNHESAG-TLVPR--------------------      519
hSERT  IKSITPETPTEIPCGDIRLNA--------------------      629
dDAT   TILTTPWRDQQSMAMVLNGVTTEVTVVRLTDTETAKEPVDV      631
hDAT   AYAIAPEKDRELVD---RGEVRQFTLRHWLKV---------      620
               :
```

Fig. S1. Sequence alignment among human dopamine transporter (hDAT), *Drosophila melanogaster* dopamine transporter (dDAT), bacterial homolog leucine transporter (LeuT), and human serotonin transporter (hSERT). F76, S422, and S429 from hDAT and their equivalent residues in dDAT, LeuT, and hSERT are highlighted in box.
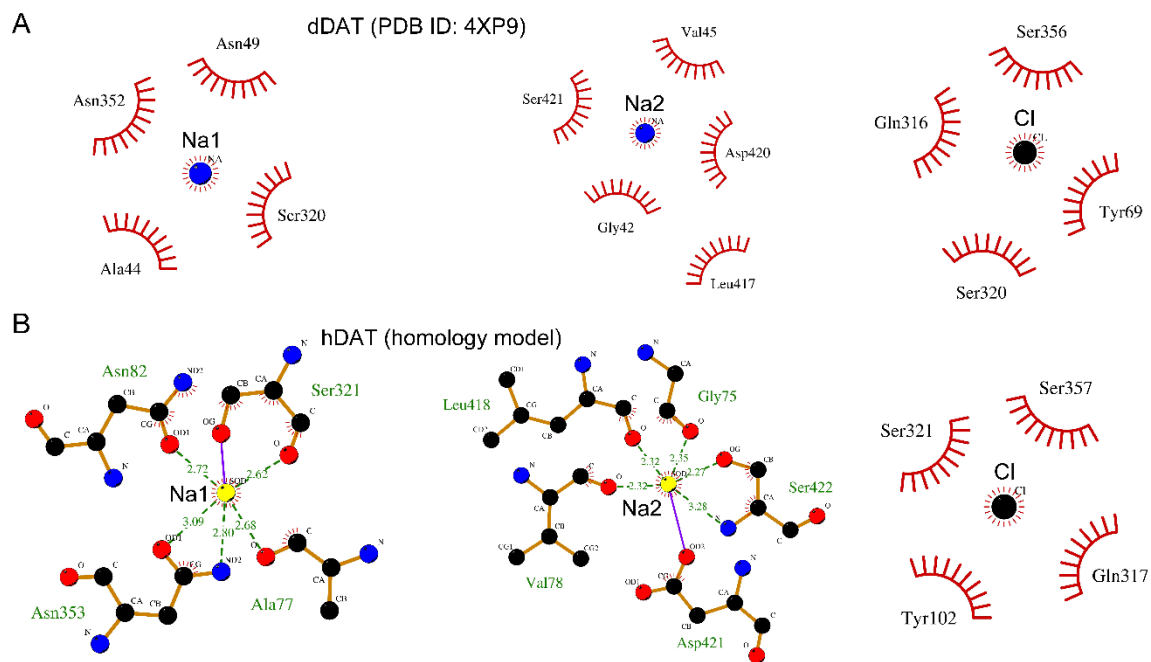
Fig. S2. Coordination sites of two Na^+ and one Cl^- ions in the dDAT (A) and hDAT (B). The equivalent sequence between dDAT and hDAT can be seen from Fig. S1. The coordinate sites of Na^+ and Cl^- was detected using LigPlot$^+$.[1]
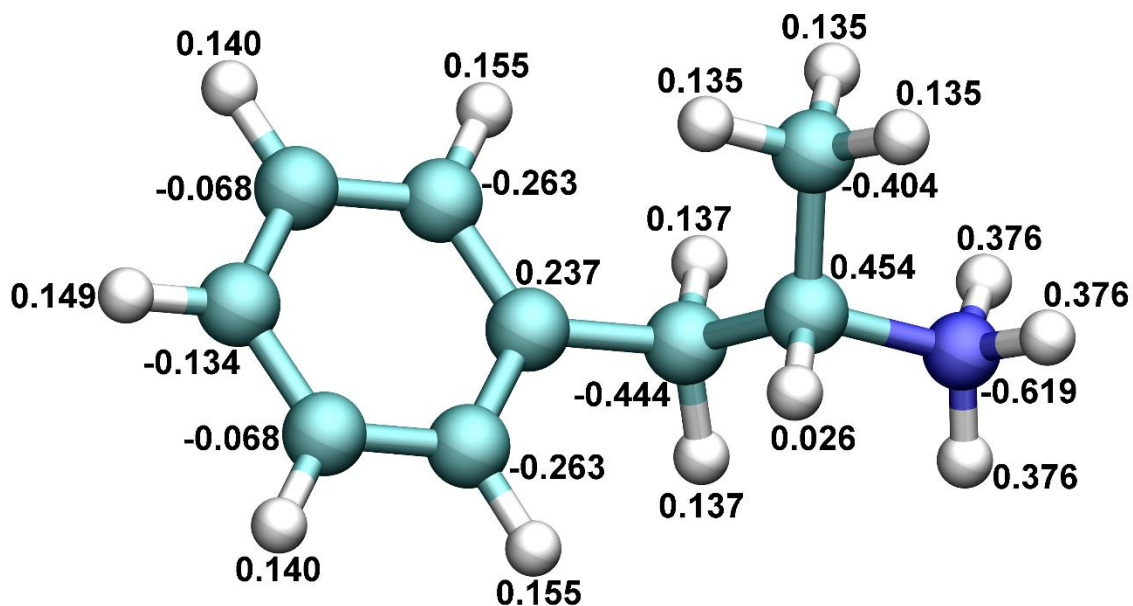
Fig. S3. RESP partial charges for AMPH molecule bearing +1e net charge. The molecular geometry of the AMPH structure was optimized at the B3LYP/6-31G* level. The electrostatic potential was calculated at the same level using the Merz-Kollma (MK) scheme. The restrained electrostatic potential (RESP) method[2] was used to fit the electrostatic potential to obtain atomic partial charges. All quantum chemical calculations were carried out using the Gaussian 03 software.[3]
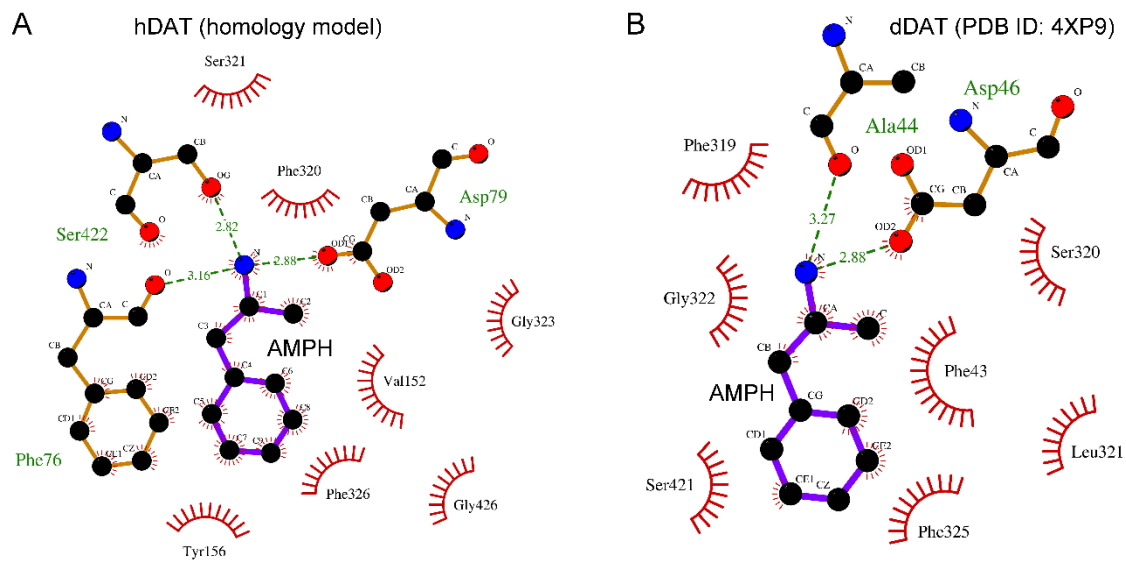
Fig. S4. The initial binding sites of AMPH in hDAT (A) and dDAT (B). The equivalent sequence between dDAT and hDAT can be seen from Fig. S1. The binding site of AMPH in dDAT were taken from the crystal structure of dDAT (PDB ID: 4XP9). The binding sites of AMPH were detected using LigPlot+.[1]
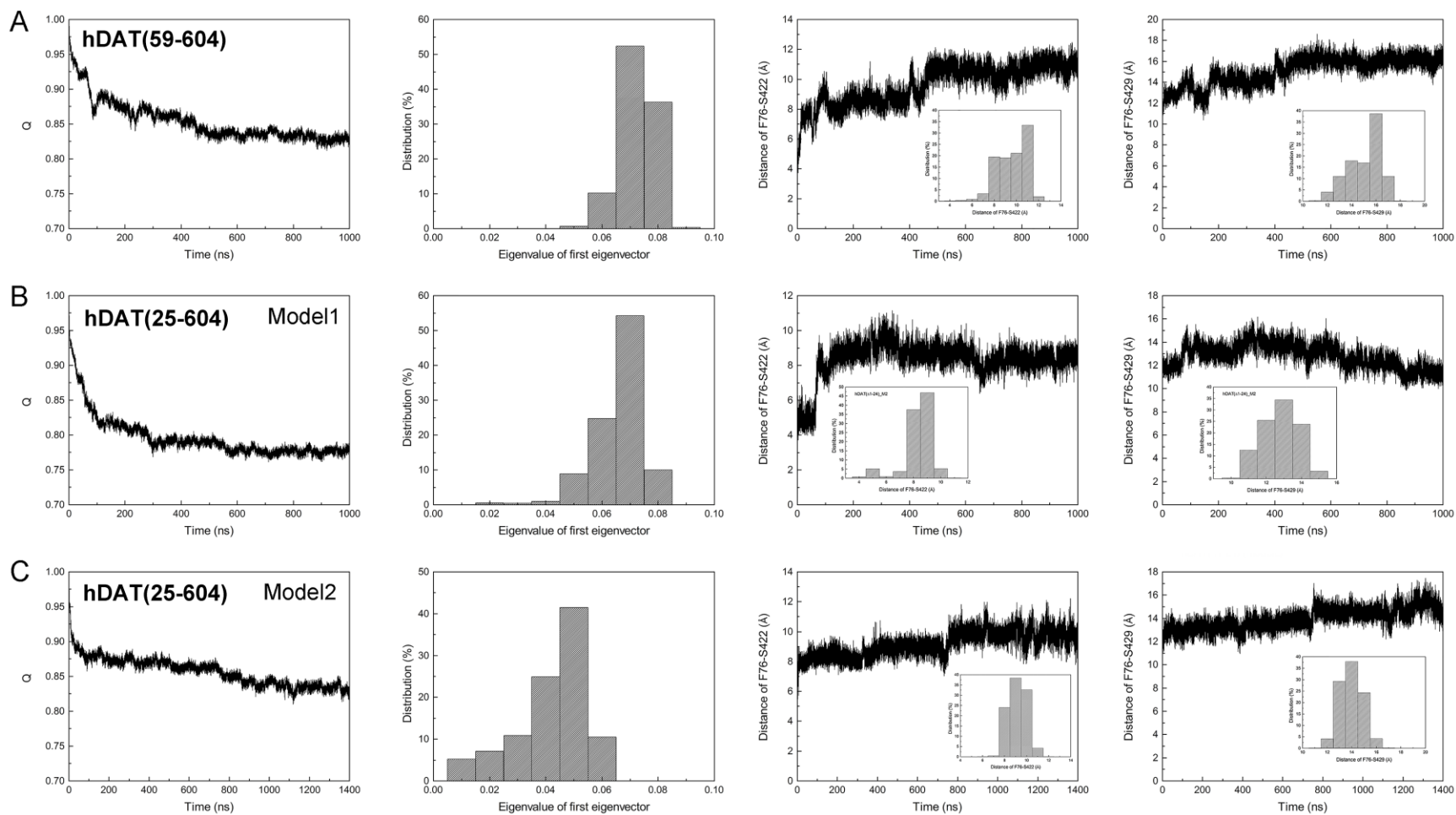
Fig. S5. Results (the fraction of native contacts, the GNM model, the distance between Phe76 and Ser422, and the distance between Phe76 and Ser429) of truncated hDAT. (A) Results of hDAT(59–604); (B) Results of the Model 1 of hDAT(25–604); and (C) Results of the Model 2 of hDAT(25–604). The distribution of the distance is shown in the inset of each figure. Model1 and Model2 correspond to the structural models shown in Figure 1 of the main text.
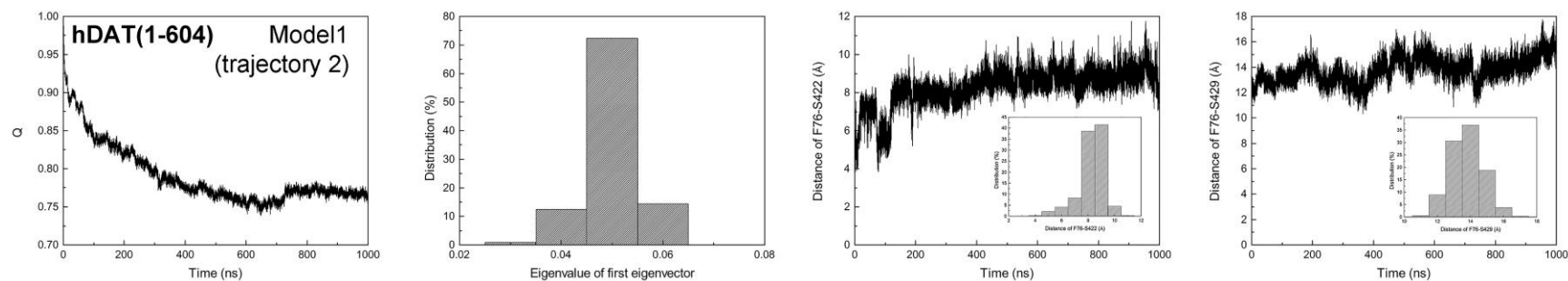
Fig. S6. Results (the fraction of native contacts, the GNM model, the distance between Phe76 and Ser422, and the distance between Phe76 and Ser429) of the Model 1 of hDAT(1–604). This is a repeated simulation of the Model1 of hDAT(1–604) using a different random number for the initial velocity distribution. Reproducible results were obtained: single state and inward-open state.

Fig. S7. Results (the fraction of native contacts, the GNM model, the distance between Phe76 and Ser422, and the distance between Phe76 and Ser429) of p-hDAT(1–604).

Fig. S8. Representative conformations of p-hDAT($1-604$) over 1-μs MD simulations from side and intracellular views for Model1 and Model 2. The five serine residues and two truncation points (V24 and Q58) are labeled. The N-terminal region is colored in red and the TM1a and TM6a are colored in blue. Model1 and Model2 correspond to the structural models shown in Figure 1 of the main text.

Fig. S9. Results (the fraction of native contacts, the GNM model, the distance between Phe76 and Ser422, and the distance between Phe76 and Ser429) of the Model 1 of p-hDAT(1–604) (A) and Model2 of p-hDAT(1–604) (B). These are repeated simulations of the two models of p-hDAT(1–604) using a different random number for the initial velocity distribution. Note that the conformational states (either outward-facing or inward-facing) are defined by the transmembrane domains, however, the presence of N-terminal tail, especially the phosphorylated N-terminal, may introduce noise for the calculation of the relative distribution of conformational states. To test this, we calculated the state distribution involving TM domains (residues 60–604) only, and showed results in (C). A dominant single state was found for both models of p-hDAT(1–604). For AMPH-bound hDAT(25–604) (**Fig. S10D**), and AMP-bound p-hDAT(1–604), we also observed the same effect of N-terminal on the state distribution (**Fig. S13**). Of interest, the N-terminal regions in these systems display various types of β-strands (**Fig. S22** and **Fig. S27**)
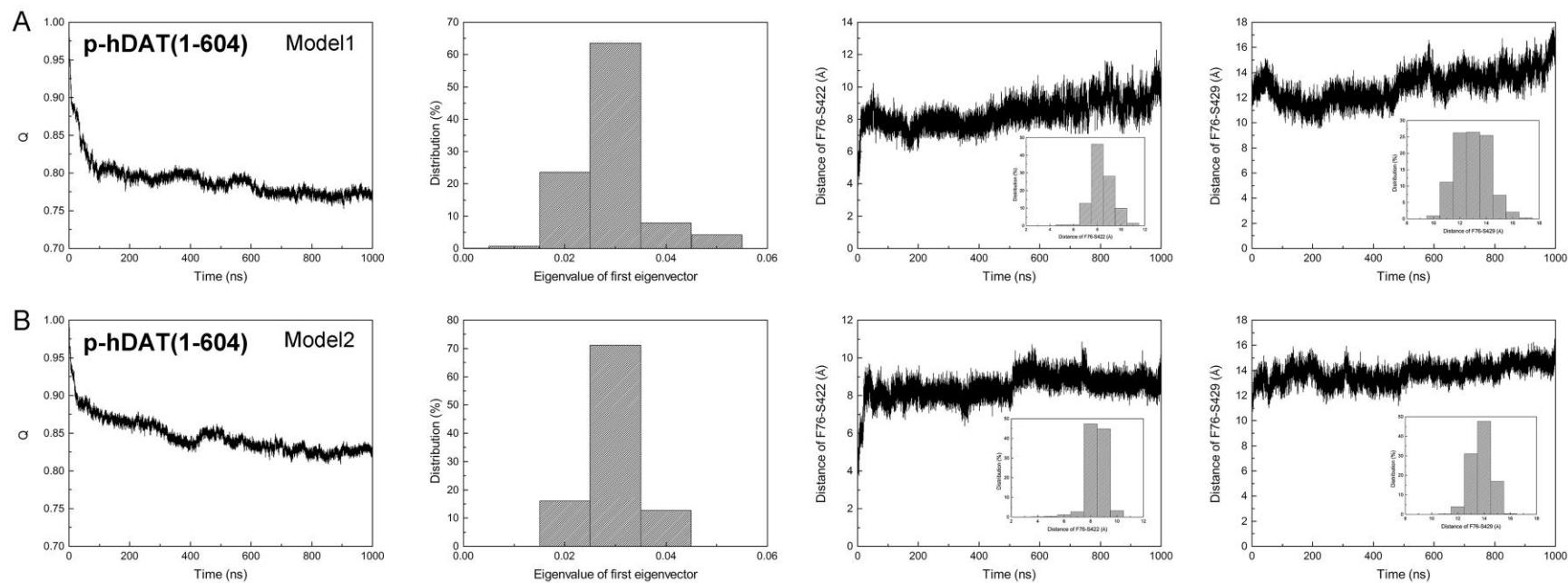
Fig. S10. Results (the fraction of native contacts, the GNM model, the distance between Phe76 and Ser422, and the distance between Phe76 and Ser429) of truncated hDAT in complex with AMPH. (A) Results of AMPH-bound hDAT(59–604); (B) Results of the Model1 of AMPH-bound hDAT(25–604); (C) Results of the Model2 of AMPH-bound hDAT(25–604); and (D) The state distribution calculated for TM domains (residues 60–604) only. The distribution of the distance is shown in the inset of each figure. Model1 and Model2 correspond to the structural models shown in Figure 1 of the main text.
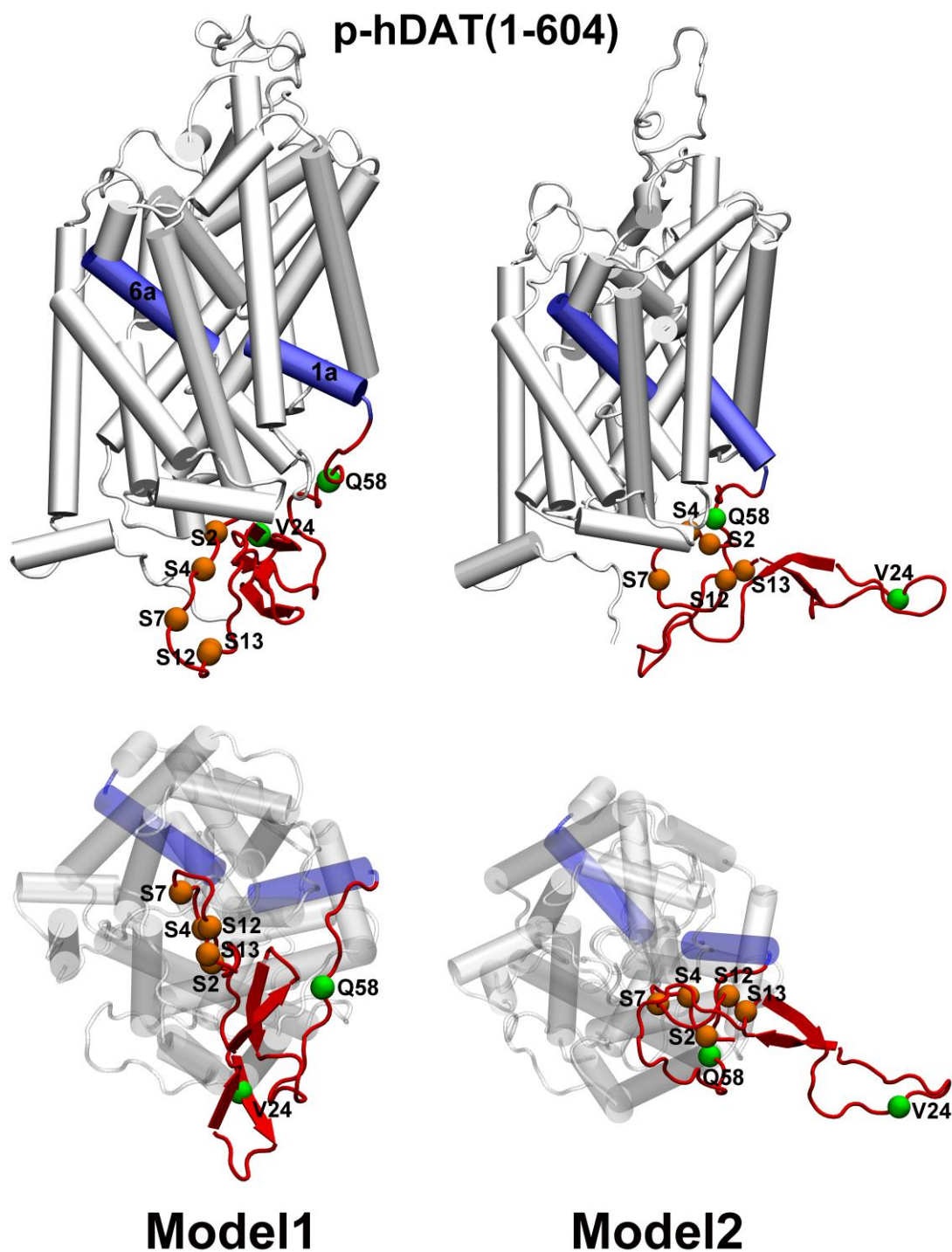
Fig. S11. Results (the fraction of native contacts, the GNM model, the distance between Phe76 and Ser422, and the distance between Phe76 and Ser429) of AMPH-bound hDAT(59–604). This is a repeated simulation of hDAT(59–604) in complex with AMPH using a different random number for the initial velocity distribution. Reproducible results were obtained: single state and outward-open state.
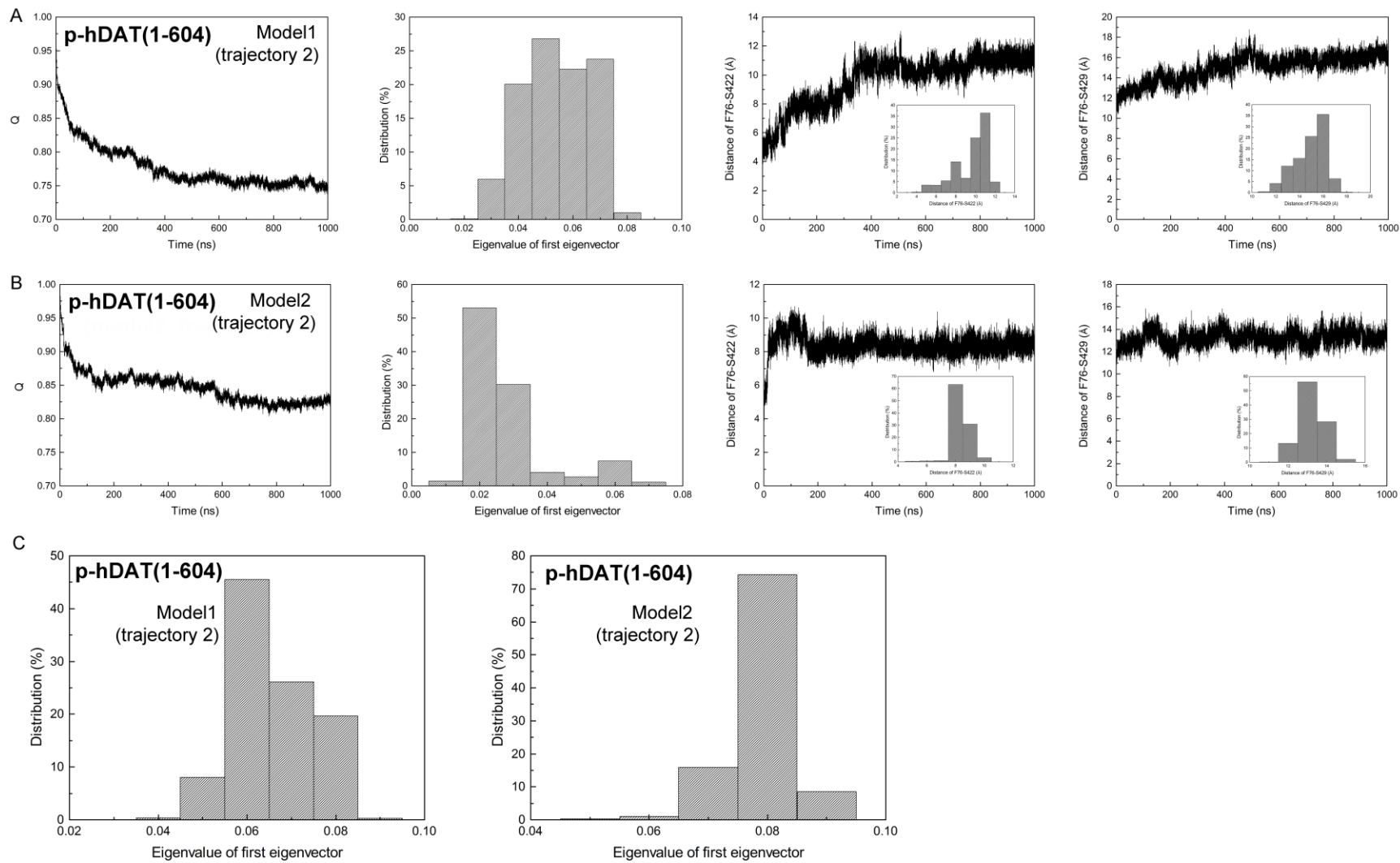
Fig. S12. Results (the fraction of native contacts, the GNM model, the distance between Phe76 and Ser422, and the distance between Phe76 and Ser429) of AMPH-bound hDAT(1–604). (A) Results of the Model1 of AMPH-bound hDAT(1–604); and (B) Results of the Model2 of AMPH-bound hDAT(1–604). The distribution of the distance is shown in the inset of each figure. Model1 and Model2 correspond to the structural models shown in Figure 1 of the main text.
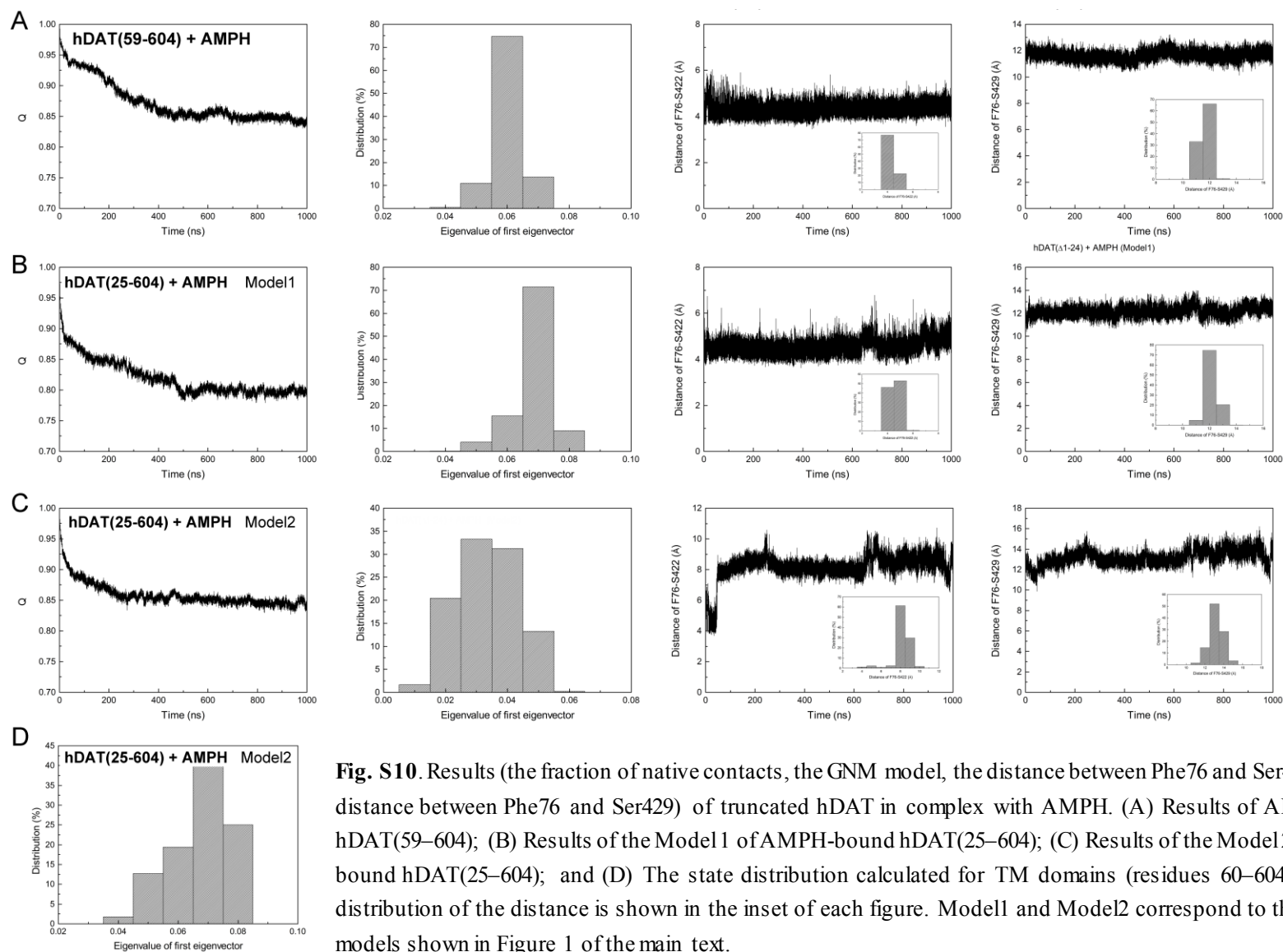
Fig. S13. Results (the fraction of native contacts, the GNM model, the distance between Phe76 and Ser422, and the distance between Phe76 and Ser429) of AMPH-bound p-h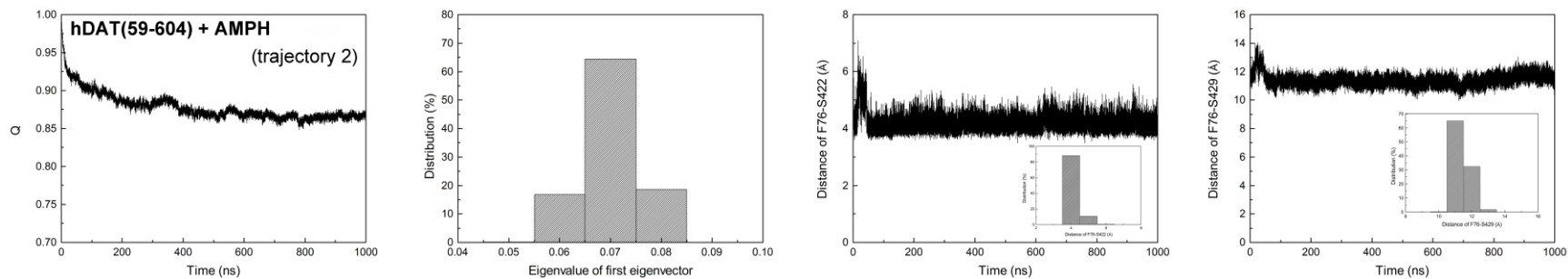DAT(1–604). (A) Results of the Model1 of AMPH-bound p-hDAT(1–604); (B) Results of the Model 2 of AMPH-bound p-hDAT(1–604); and (C) The state distribution calculated for TM domains (residues 60–604) only. For details, see **Fig. S9**. The distribution of the distance is shown in the inset of each figure. Model1 and Model2 correspond to the structural models shown in Figure 1 of the main text.
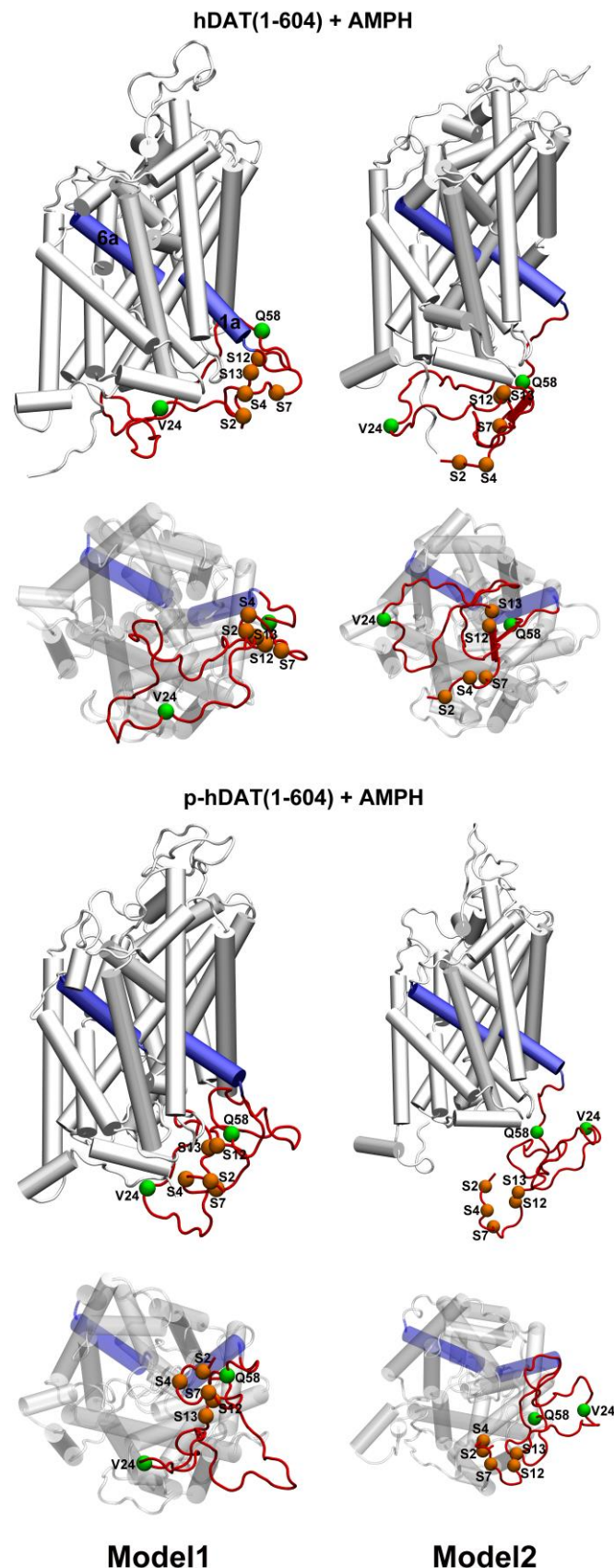
Fig. S14. Representative conformations of hDAT(1–604) in complex with AMPH and p-hDAT(1–604) in complex with AMPH over 1-μs MD simulations from side and intracellular views for Model1 and Model 2. The five serine residues and two truncation points (V24 and Q58) are labeled. The N-terminal region is colored in red and the TM1a and TM6a are colored in blue. Model1 and Model2 correspond to the structural models shown in Figure 1 of main text.
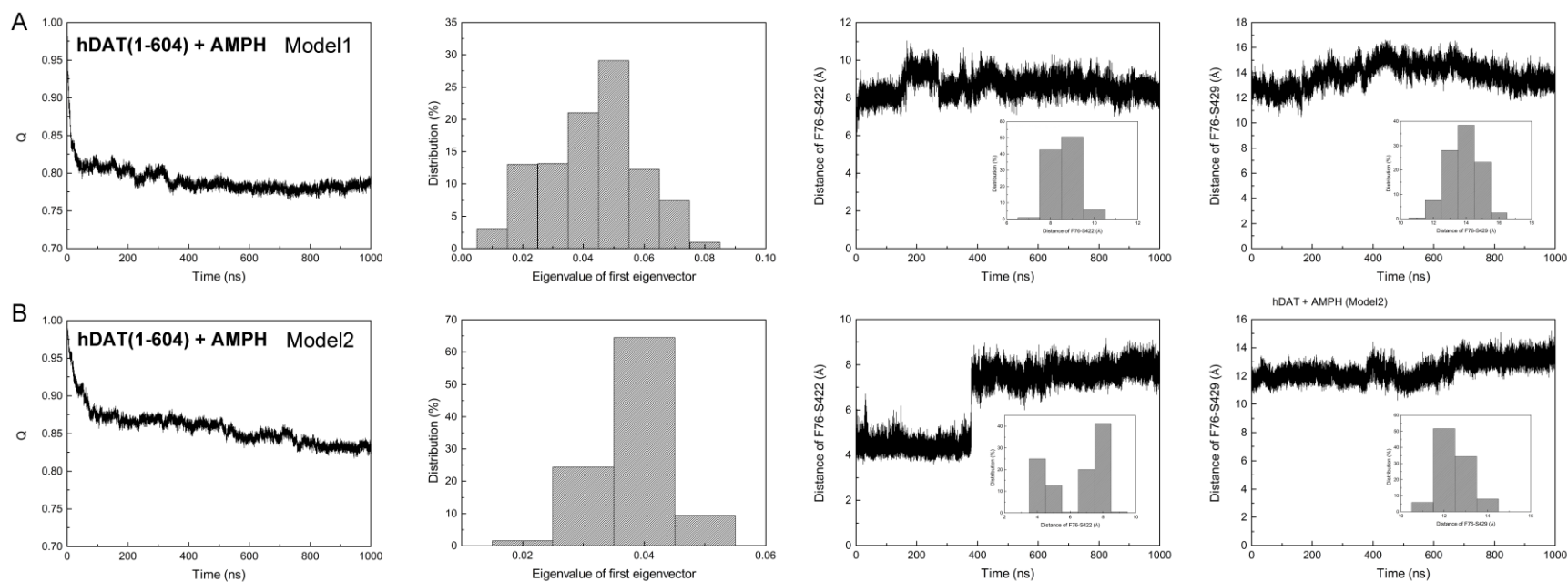
S17
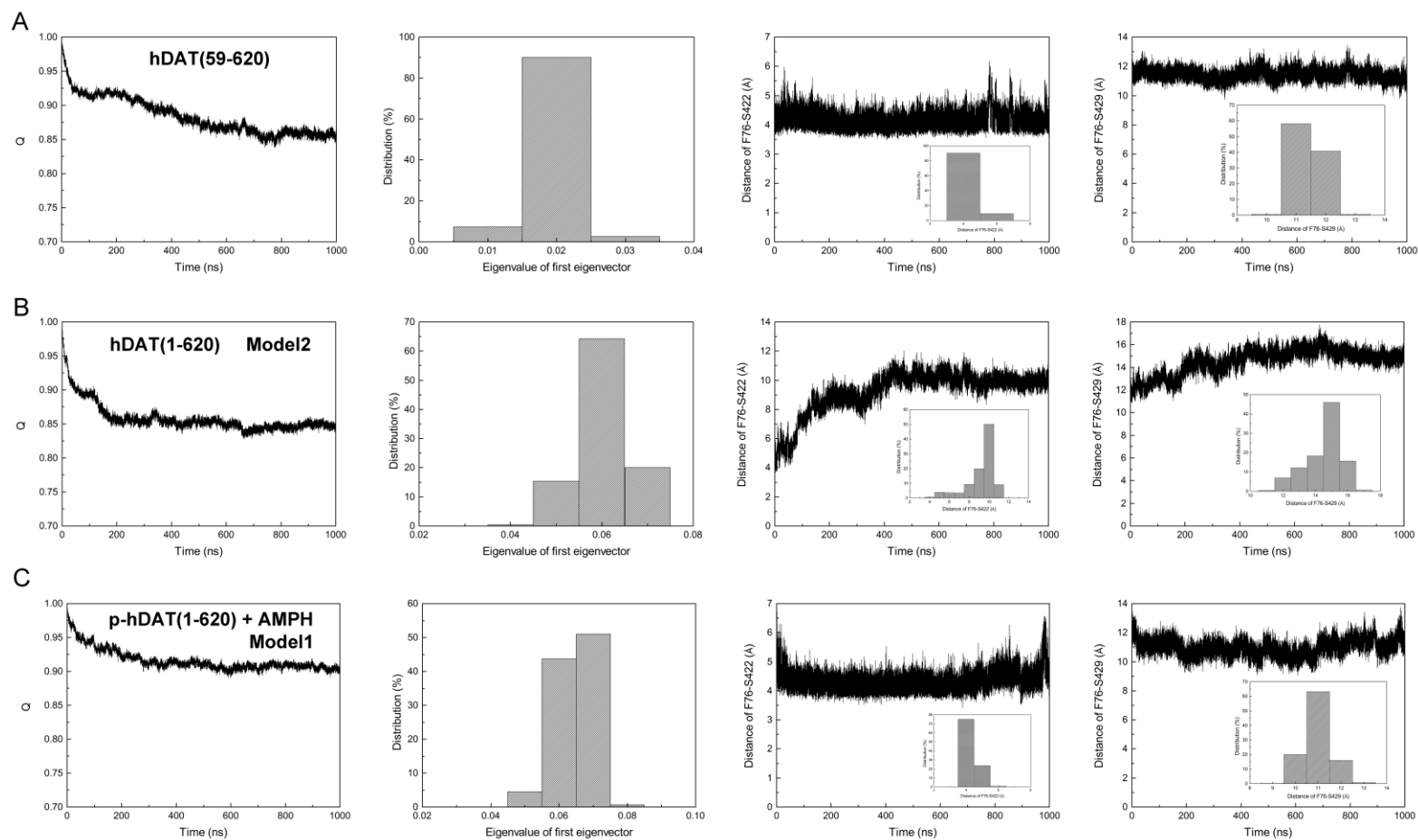
Fig. S15. Results (the fraction of native contacts, the GNM model, the distance between Phe76 and Ser422, and the distance between Phe76 and Ser429). (A) Results of hDAT(59–620); (B) Results of the Model2 of hDAT(1–620); and (C) Results of the Model 1 of p-hDAT(1–620) in complex with AMPH. The distribution of the distance is shown in the inset of each figure. Model1 and Model2 correspond to the structural models shown in Figure 1 of the main text.
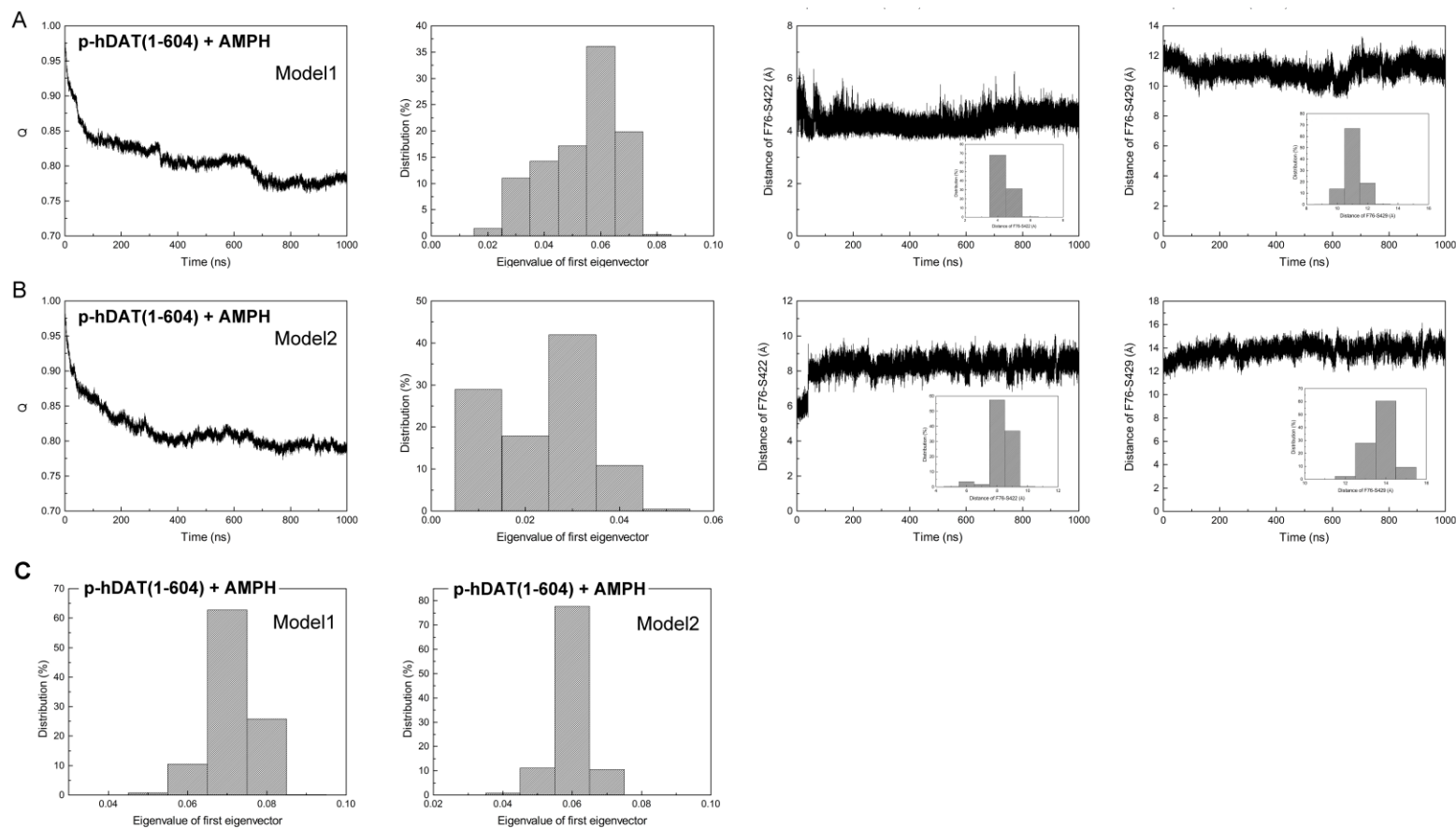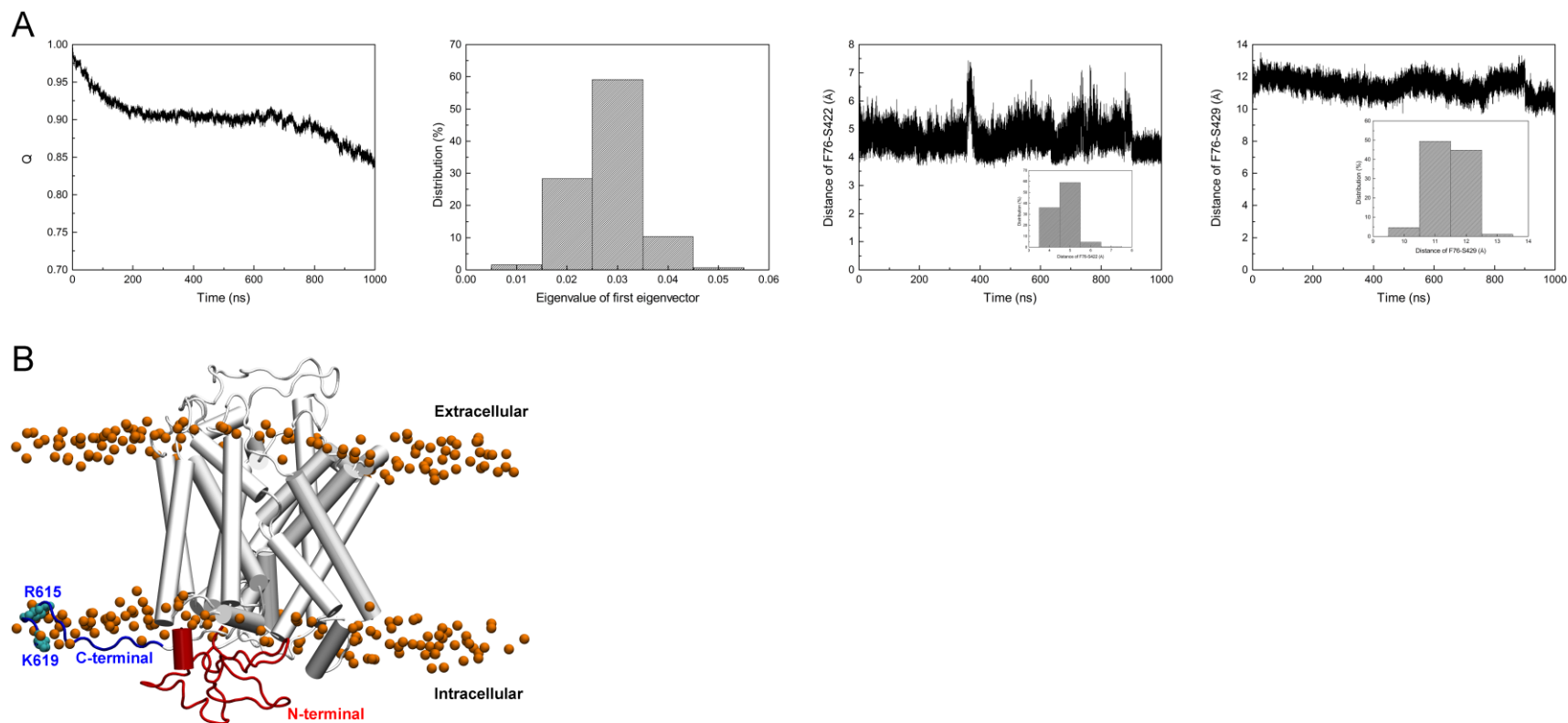
Fig. S16. (A) Results (the fraction of native contacts, the GNM model, the distance between Phe76 and Ser422, and the distance between Phe76 and Ser429). of the designed full-length hDAT; (B) Representative conformation of this full-length hDAT in membrane. Note that the C-terminal tail was restrained by electrostatic interactions (Arg615 and Lys619) with lipid head groups, and thus preventing the interactions between the N-terminal and C-terminal regions. As a result, the designed hDAT remained in the outward-open state.

Table S1. Summary of angels (in degree, peak values) between TM1a and TM6a with respect to z-axis. The angels correspond to the outward-facing (<mark>OF</mark>) states are highlighted in yellow. For details, see Figs. S17–S20.

System	hDAT		hDAT + AMPH	
	TM1a	TM6a	TM1a	TM6a
hDAT(59−604)	28	142	<mark>18</mark>	<mark>145</mark>
hDAT(25−604) (Model1)	39	153	<mark>28</mark>	<mark>146</mark>
hDAT(25−604) (Model2)	26	146	22	142
hDAT(1−604) (Model1)	10	146	13	143
hDAT(1−604) (Model2)	<mark>19</mark>	<mark>138</mark>	23	147
p-hDAT(1−604) (Model1)	32	146	<mark>29</mark>	<mark>142</mark>
p-hDAT(1−604) (Model2)	13	146	21	146
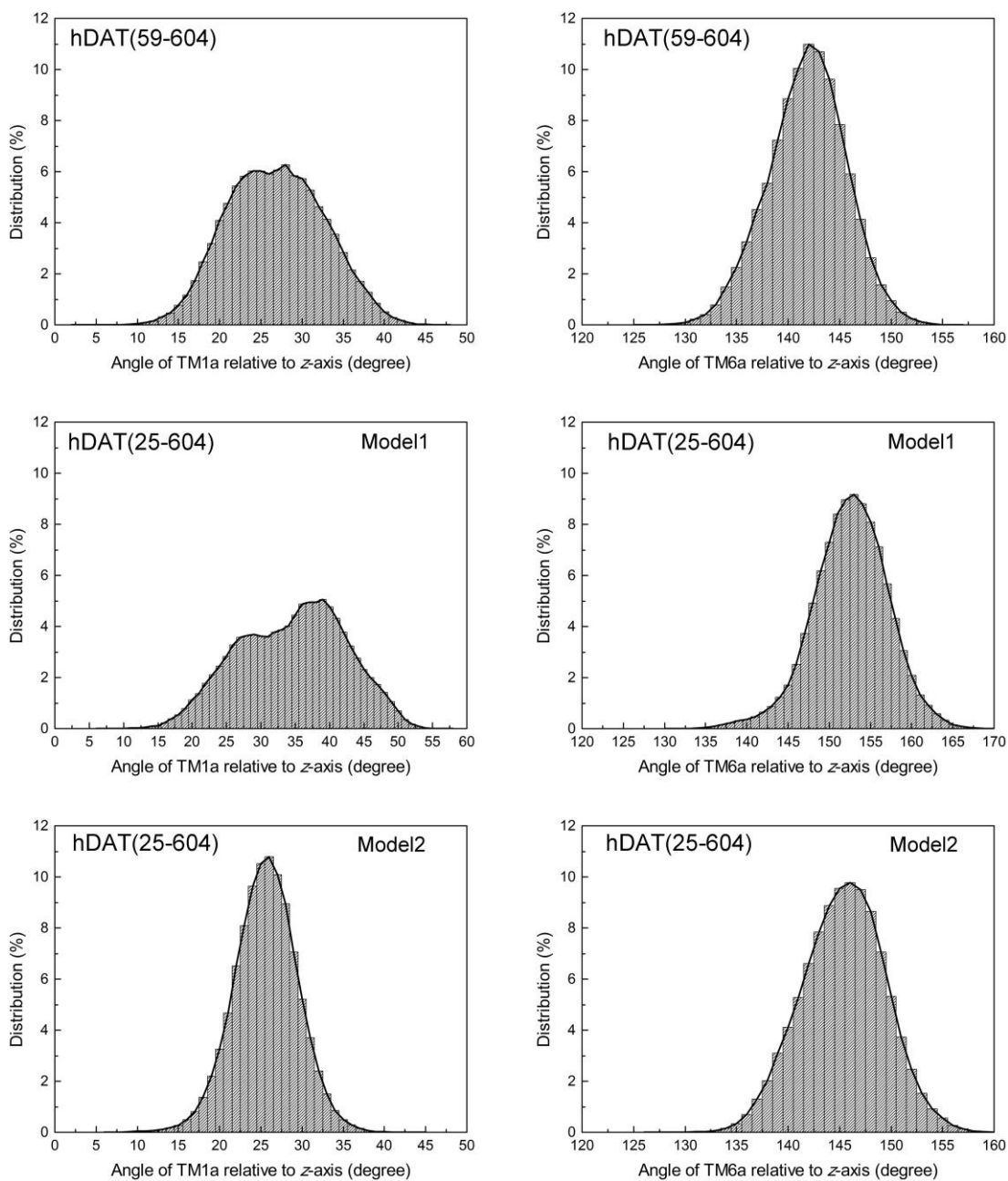
Fig. S17. Distribution of angels of TM1a and TM6a with respect to z-axis in truncated hDAT. Model1 and Model2 correspond to the initial models of hDAT show Figure 1 of main text.
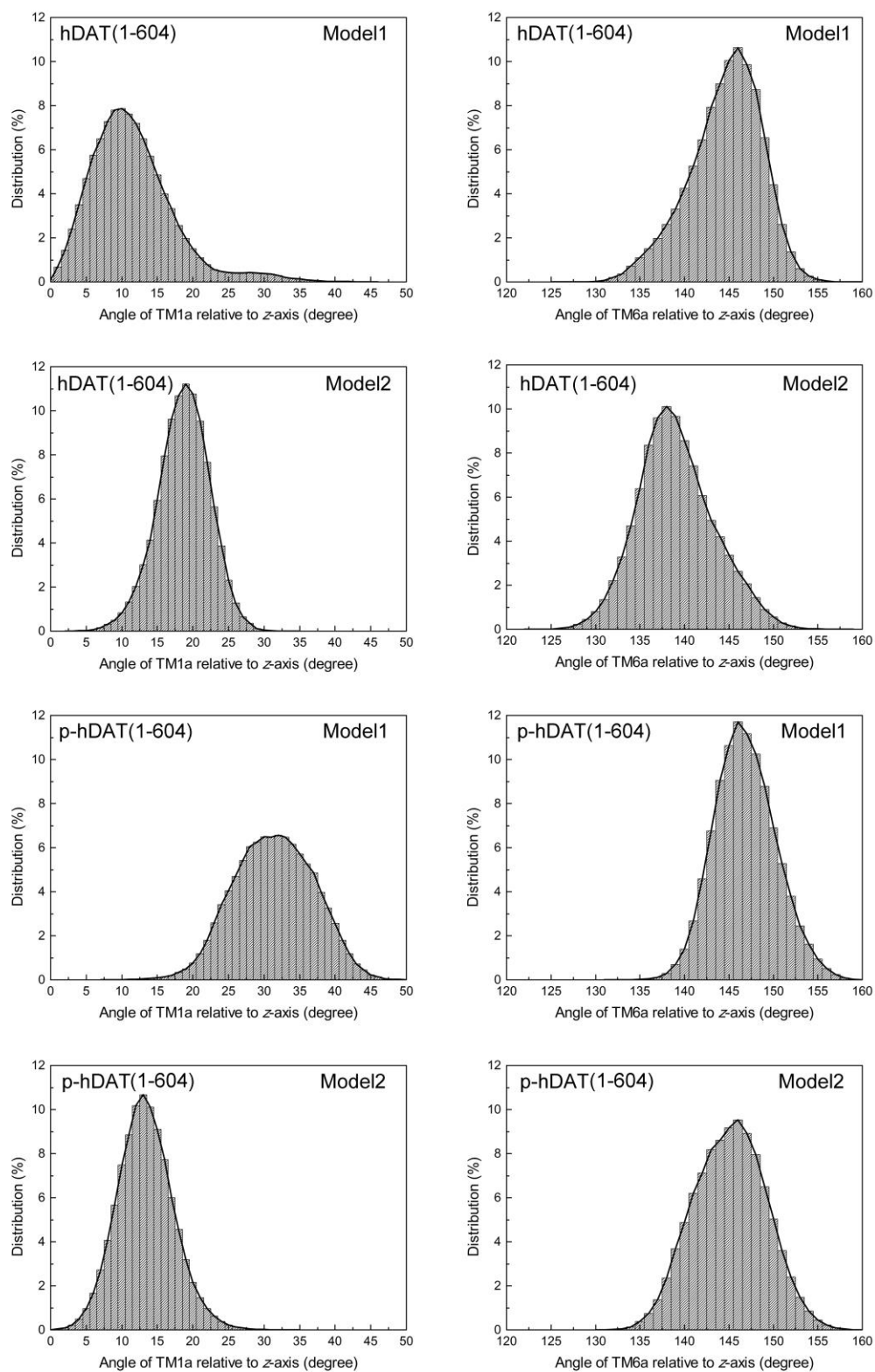
Fig. S18. Distribution of angels of TM1a and TM6a with respect to z-axis in hDAT and p-hDAT.
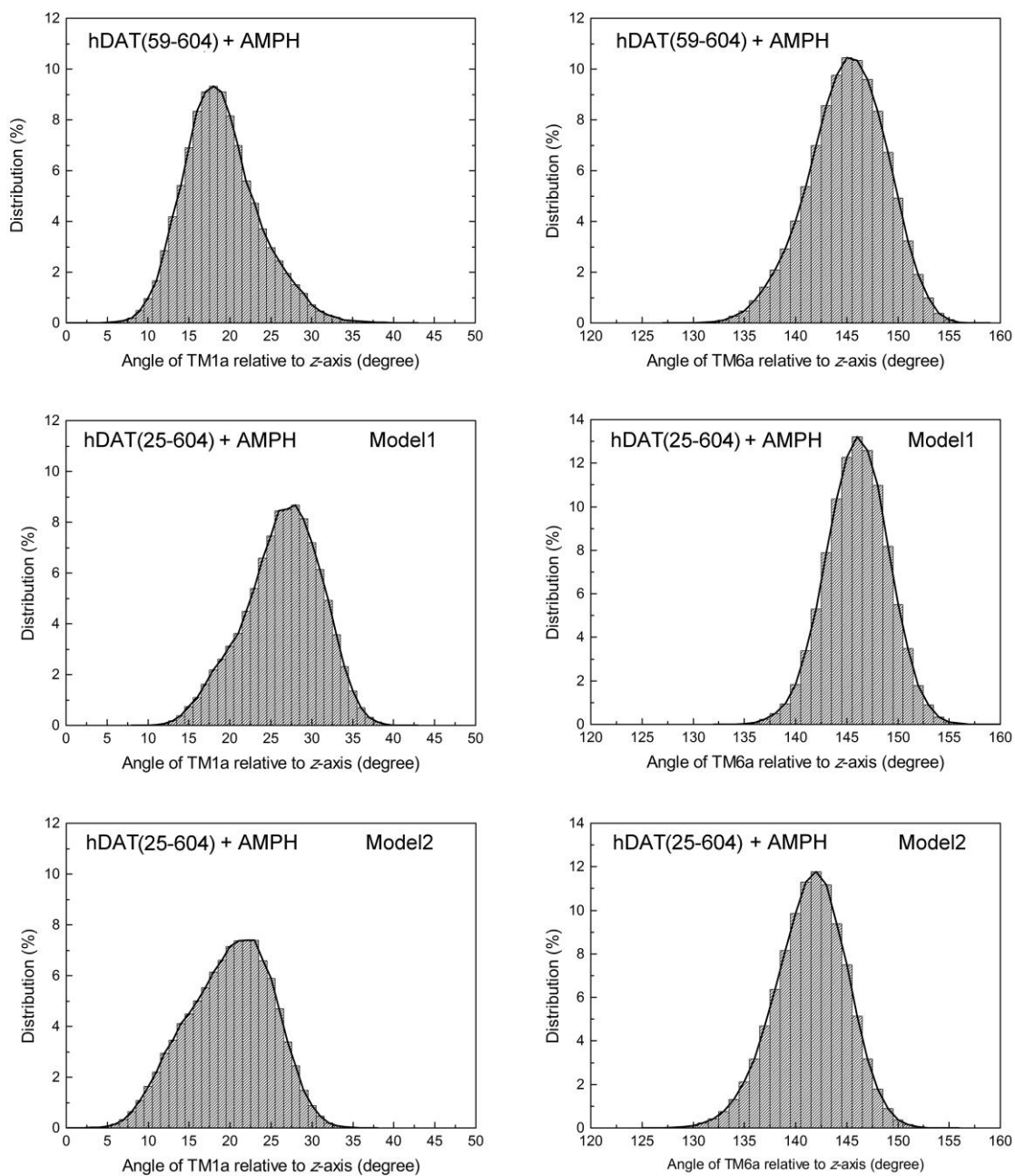
Fig. S19. Distribution of angels of TM1a and TM6a with respect to z-axis in truncated hDAT in complex with AMPH.
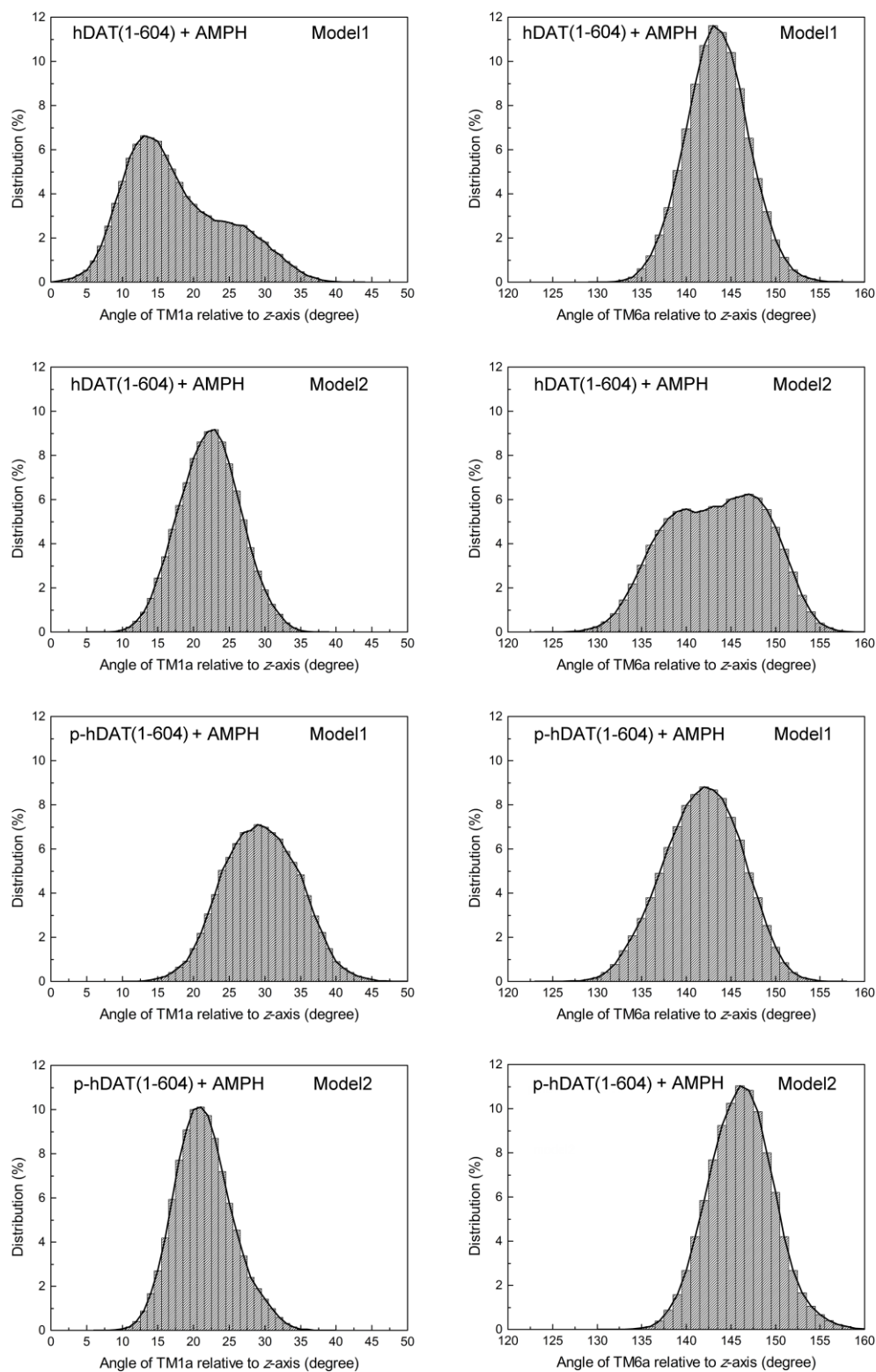
Fig. S20. Distribution of angels of TM1a and TM6a with respect to z-axis in AMPH-bound hDAT and p-hDAT.
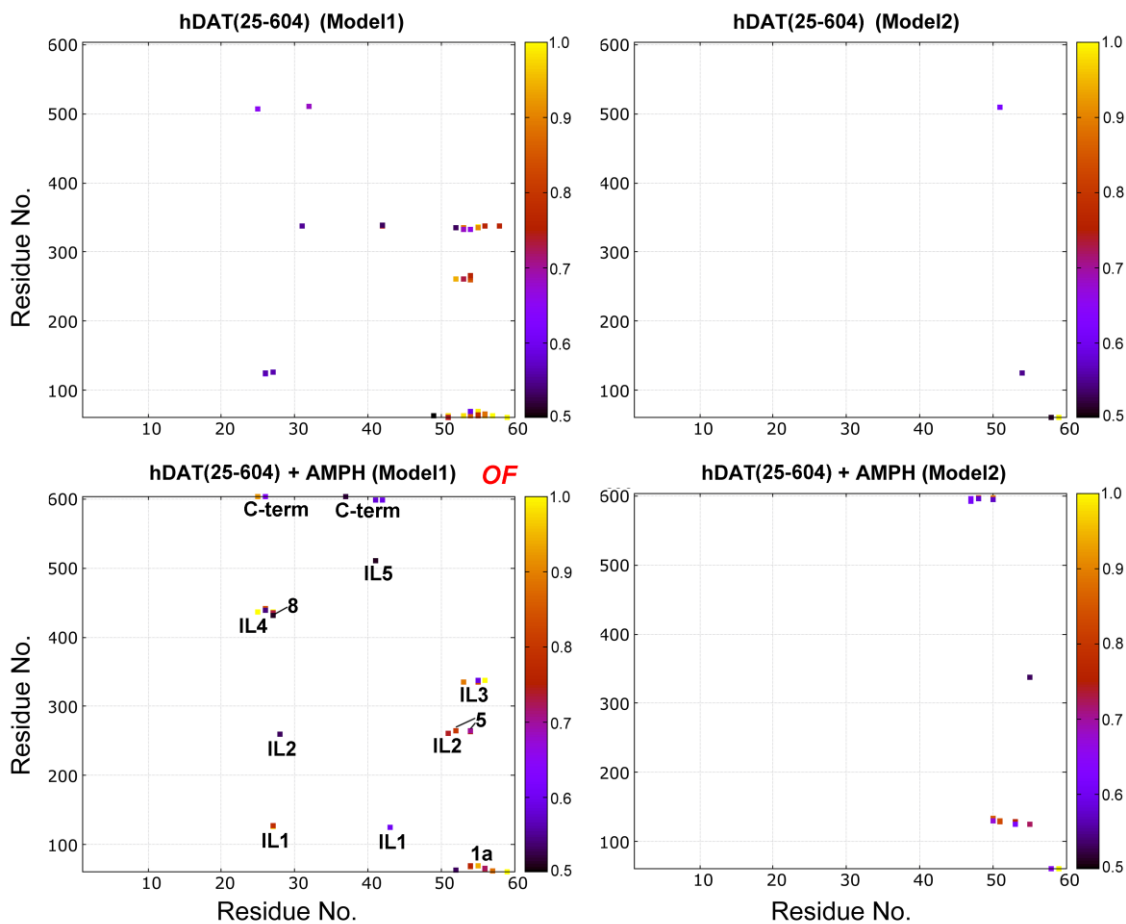
Fig. S21. Computed contact maps between residues in the N-terminal and intracellular region of hDAT(25–604) and AMPH-bound hDAT(25–604) models. A contact occurs if any atom in the N-terminal region is within 3 Å of any atom in the TM domains, and only a contact frequency >0.5 (50%) is shown. For electrostatic interactions, see Table S2. Contact frequency was calculated using the last 500-ns trajectory of each system. **OF** denotes the outward-facing open state.

Table S2. Contact frequency calculated for short-range electrostatic interactions between residues in the N-terminal and in the intracellular region. IF and OF indicate inward-facing and outward-facing state, respectively. For details, see Fig. S21.

hDAT(25–604) (Model1, IF)			hDAT (25–604) (Model2, IF)		
Residue in NT	Residue in TMs	Contact Frequency	Residue in NT	Residue in TMs	Contact Frequency
Arg51	Asp59	0.88	No contact frequency > 0.5 was found		
Glu56	Lys65	0.88			
Arg51	Arg60	0.79			
Glu56	Lys337	0.76			
Arg51	Glu61	0.74			
Lys27	Glu126	0.56			
hDAT(25–604) + AMPH (Model1, OF)			**hDAT(25–604) + AMPH (Model2, IF)**		
Residue in NT	Residue in TMs	Contact Frequency	Residue in NT	Residue in TMs	Contact Frequency
Lys27	Asp436	1.00	No contact frequency > 0.5 was found		
Glu56	Lys337	1.00			
Lys27	Glu126	0.96			
Glu56	Lys65	0.77			
Glu56	Lys66	0.72			
Glu28	Lys260	0.53			
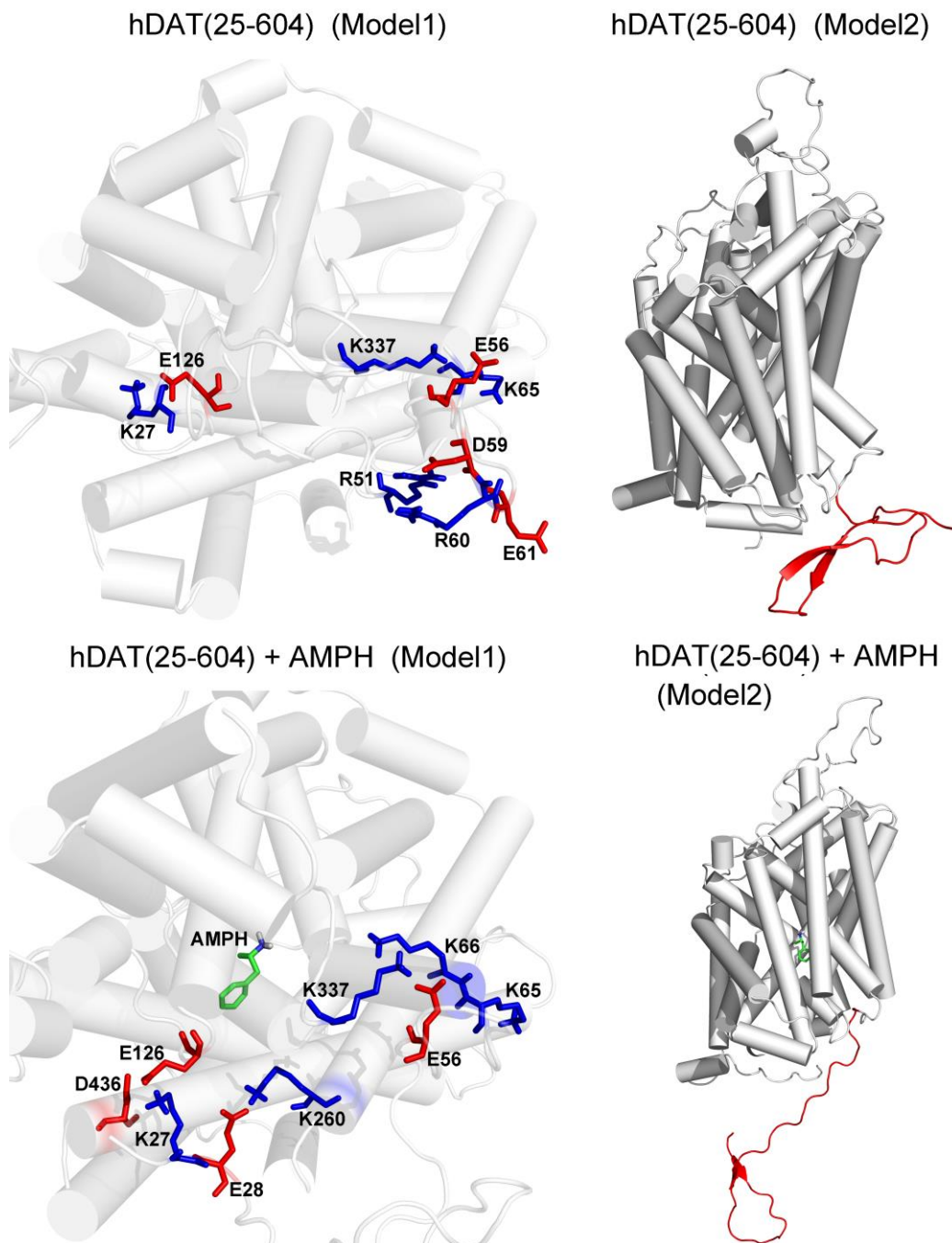
Fig. S22. Electrostatic network for hDAT(25–604) and AMPH-bound hDAT(25–604) models. For the contact frequency, see Table S2.
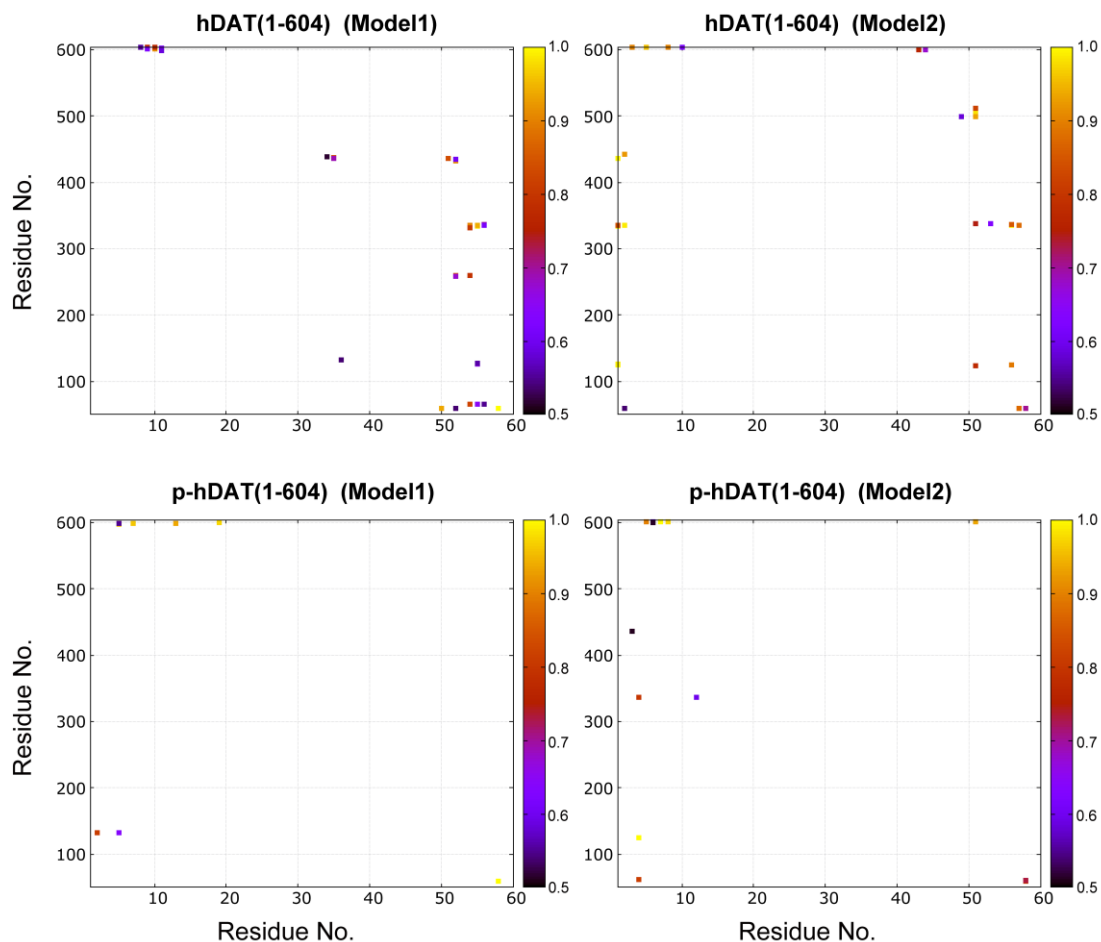
Fig. S23. Computed contact maps between residues in the N-terminal and the intracellular region of hDAT(1–604) and p-hDAT(1–604) models. A contact occurs if any atom in the N-terminal region is within 3 Å of any atom in the TM domains, and only a contact frequency >0.5 (50%) is shown. For electrostatic interactions, see Table S3. Contact frequency was calculated using the last 500-ns trajectory of each system. The contact maps for hDAT(1–604) models are the same as shown in Figure 4a and 4b of main text.
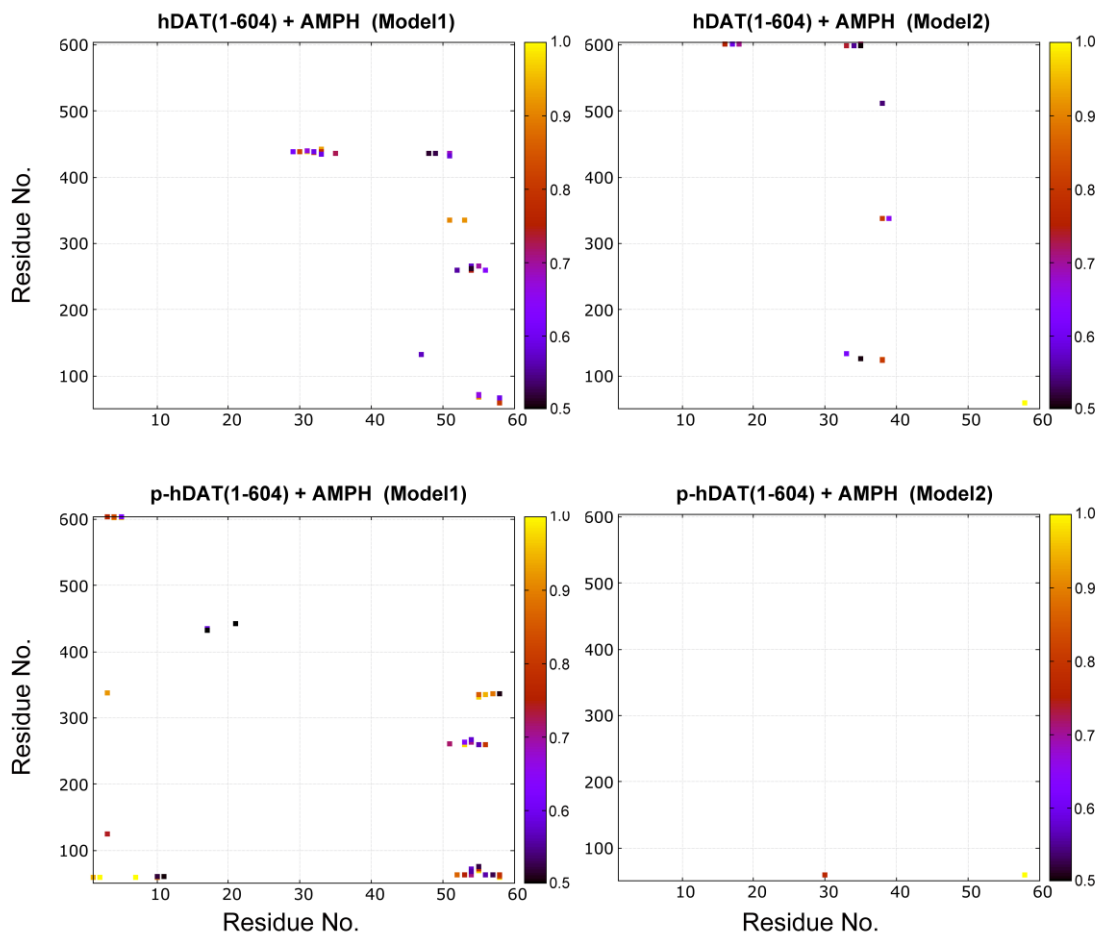
Fig. S24. Computed contact maps between residues in the N-terminal and the intracellular region of AMPH-bound hDAT(1–604) and AMPH-bound p-hDAT(1–604). A contact occurs if any atom in the N-terminal region is within 3 Å of any atom in the TM domains, and only a contact frequency >0.5 (50%) is shown. For electrostatic interactions, see Table S3. Contact frequency was calculated using the last 500-ns trajectory of each system. The contact maps for AMPH-bound p-hDAT(1–604) models are the same as shown in Figure 4c and 4d of main text.

Table S3. Contact frequency calculated for short-range electrostatic interactions between residues in the N-terminal and in the intracellular region of hDAT, p-hDAT. AMPH-bound hDAT, and AMPH-bound p-hDAT. IF and OF indicate inward-facing and outward-facing state, respectively. For details, see Figs. S24–S26.

hDAT(1−604) (Model1, IF)			hDAT(1−604) (Model2, OF)		
Residue in NT	Residue in TMs	Contact Frequency	Residue in NT	Residue in TMs	Contact Frequency
Arg51	Asp436	0.84	Arg51	Asp507	0.98
Lys35	Glu437	0.82	Glu56	Arg125	0.89
Glu56	Lys337	0.70	Glu56	Lys337	0.85
Lys35	Asp436	0.69			
Glu56	Lys66	0.55			
Glu36	Lys133	0.54			

p-hDAT(1−604) (Model1, IF)			p-hDAT(1−604) (Model2, IF)		
Residue in NT	Residue in TMs	Contact Frequency	Residue in NT	Residue in TMs	Contact Frequency
Lys19	Asp600	0.97	Lys5	Arg601	0.90
Lys5	Lys599	0.97	Lys3	Asp436	0.51
Lys5	Lys133	0.63	p-Ser7	Arg601	1.00
Lys5	Glu598	0.55	p-Ser4	Arg125	1.00
p-Ser7	Lys599	0.96	p-Ser4	Lys337	0.80
p-Ser13	Lys599	0.93	p-Ser12	Lys337	0.59
p-Ser2	Lys133	0.81			

hDAT(1−604) + AMPH (Model1, IF)			hDAT(1−604) + AMPH (Model2, IF)		
Residue in NT	Residue in TMs	Contact Frequency	Residue in NT	Residue in TMs	Contact Frequency
Lys35	Asp436	0.72	Lys35	Arg601	0.72
Arg51	Asp436	0.68	Lys35	Glu598	0.64
Glu56	Lys260	0.64	Lys35	Glu126	0.50
			Lys35	Lys599	0.50

p-hDAT(1−604) + AMPH (Model1, OF)			p-hDAT(1−604) + AMPH (Model2, IF)		
Residue in NT	Residue in TMs	Contact Frequency	Residue in NT	Residue in TMs	Contact Frequency
Lys5	Glu602	0.97	Glu30	Arg60	0.76
Glu56	Lys260	0.79			
Lys3	Arg125	0.74			
p-Ser2	Arg60	1.00			
p-Ser7	Arg60	1.00			
p-Ser4	Glu602	0.92			

Fig. S25. Electrostatic network for hDAT(1–604) and p-hDAT(1–604) models. For the contact frequency, see Table S3.

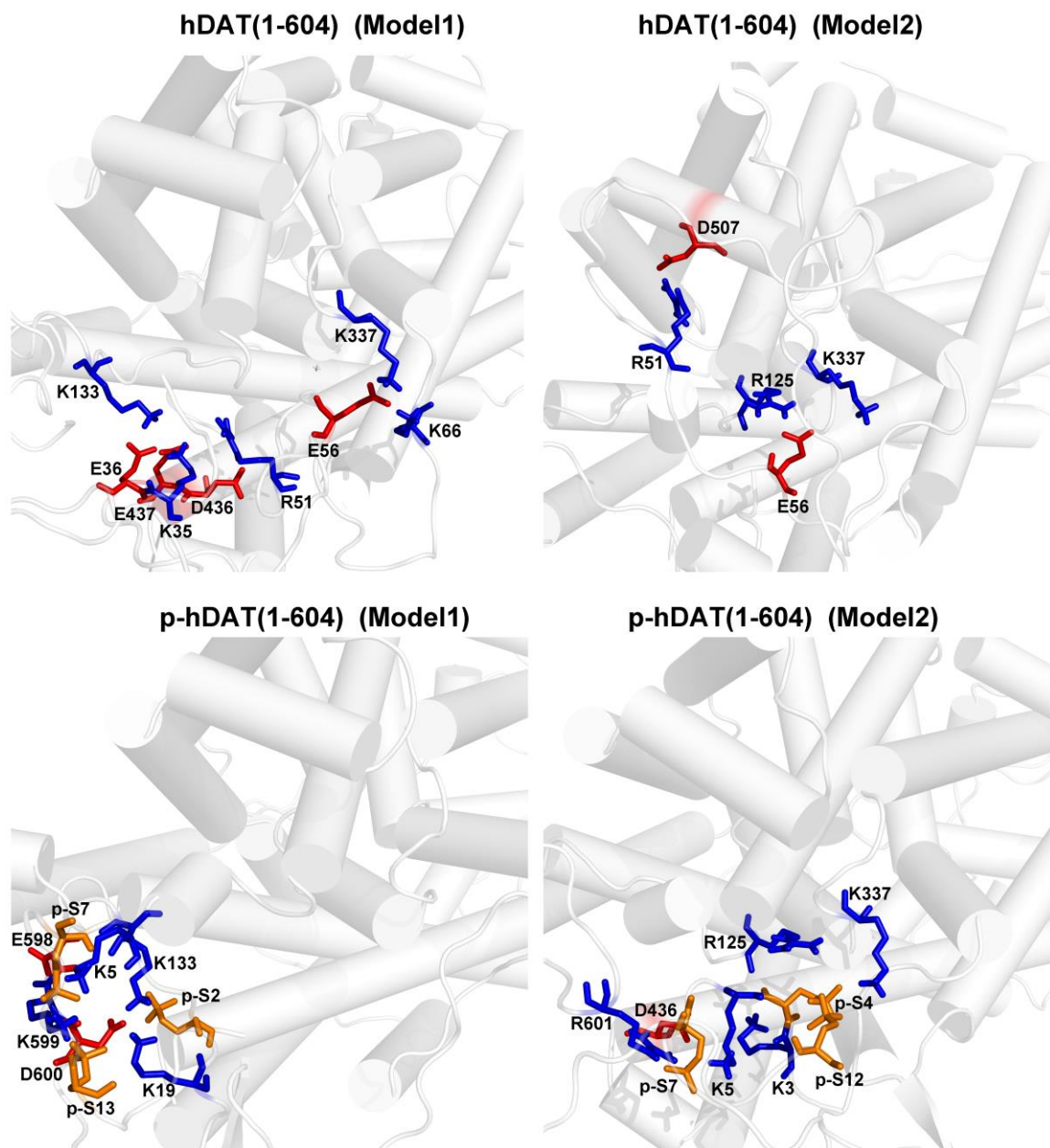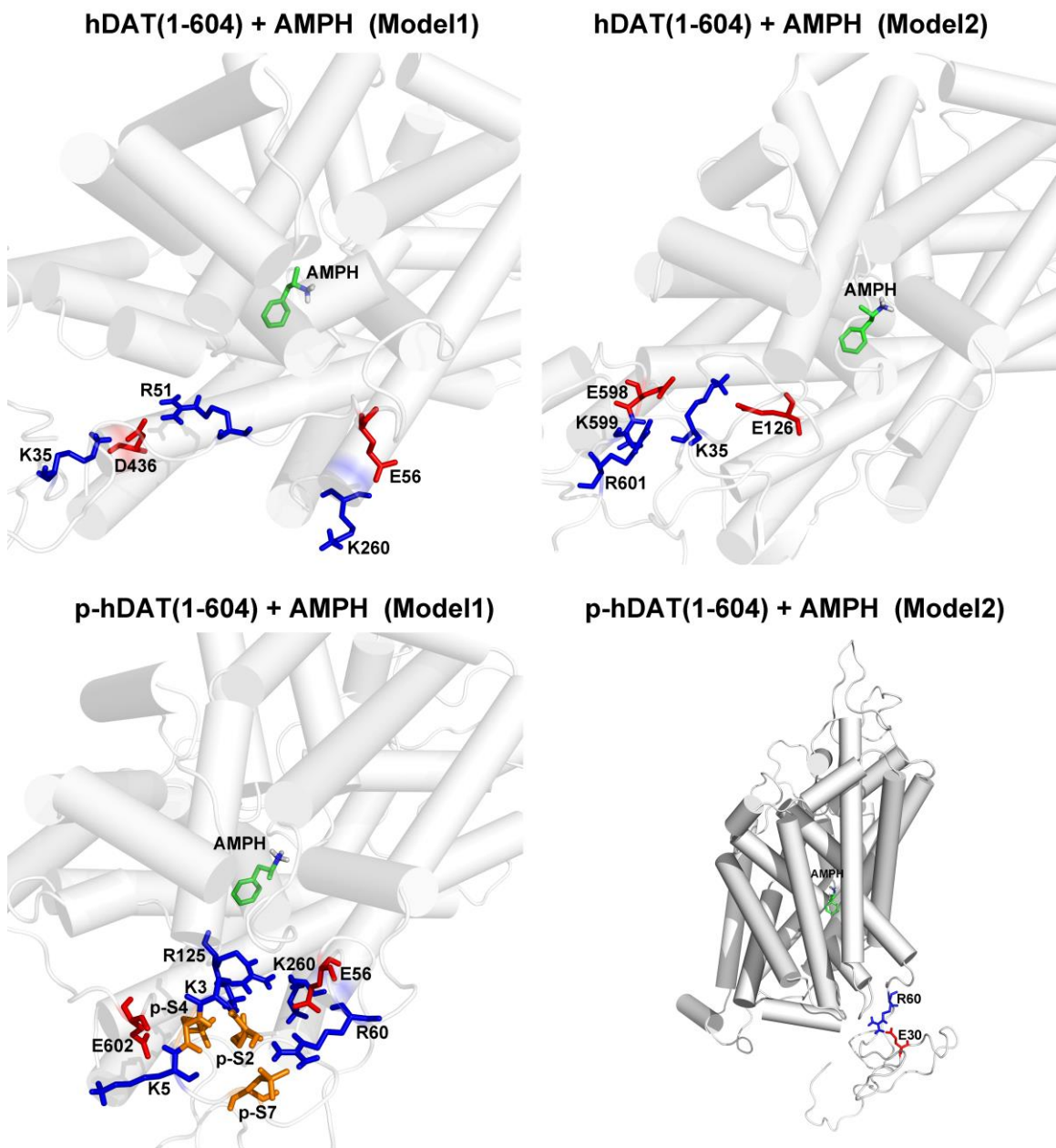**Fig. S26.** Electrostatic network for AMPH-bound hDAT(1−604) and AMPH-bound p-hDAT(1−604) models. For the contact frequency, see Table S3.

Table S4. The contact frequency between the N-terminal region and the intracellular region of AMPH-bound hDAT(25–604) (Model1, OF). IC indicates intracellular side. The electrostatic interactions are highlighted in red.

Residue in N-terminal	Residue in IC	Frequency	Assignment	Residue in N-terminal	Residue in IC	Frequency	Assignment
Ala57	Thr62	0.88	N-terminal	Val55	Tyr335	0.82	IL3
Gln52	Trp63	0.53	N-terminal	Val55	Asn336	0.93	IL3
Glu56	Gly64	0.78	N-terminal	Glu56	Lys337	1.00	IL3
Glu56	Lys65	0.77	TM1a	Val55	Lys337	0.59	IL3
Glu56	Lys66	0.72	TM1a	Lys27	Thr432	0.51	TM8
Pro54	Asp68	0.84	TM1a	Lys27	Ile435	0.73	TM8
Val55	Phe69	0.94	TM1a	Lys27	Asp436	1.00	TM8
Pro54	Phe69	0.76	TM1a	Gly25	Asp436	1.00	TM8
Thr43	Arg125	0.60	IL1	Pro26	Gln439	0.54	IL4
Lys27	Glu126	0.96	IL1	Pro26	His442	0.84	IL4
Lys27	Gly127	0.78	IL1	Gln41	Met511	0.51	IL5
Glu28	Lys260	0.53	IL2	Leu42	Lys599	0.59	C-termimal
Arg51	Thr261	0.74	IL2	Gln41	Lys599	0.58	C-termimal
Pro54	Gly263	0.77	IL2	Gly25	Val604	0.92	C-termimal
Gln52	Lys264	0.80	TM5	Pro26	Val604	0.64	C-termimal
Pro54	Lys264	0.70	TM5	Gln37	Val604	0.52	C-termimal
Ser53	Tyr335	0.89	IL3				

Table S5. The contact frequency between the N-terminal region and the intracellular region of hDAT(1–604) (Model2, OF). IC indicates intracellular side. The electrostatic interactions are highlighted in red.

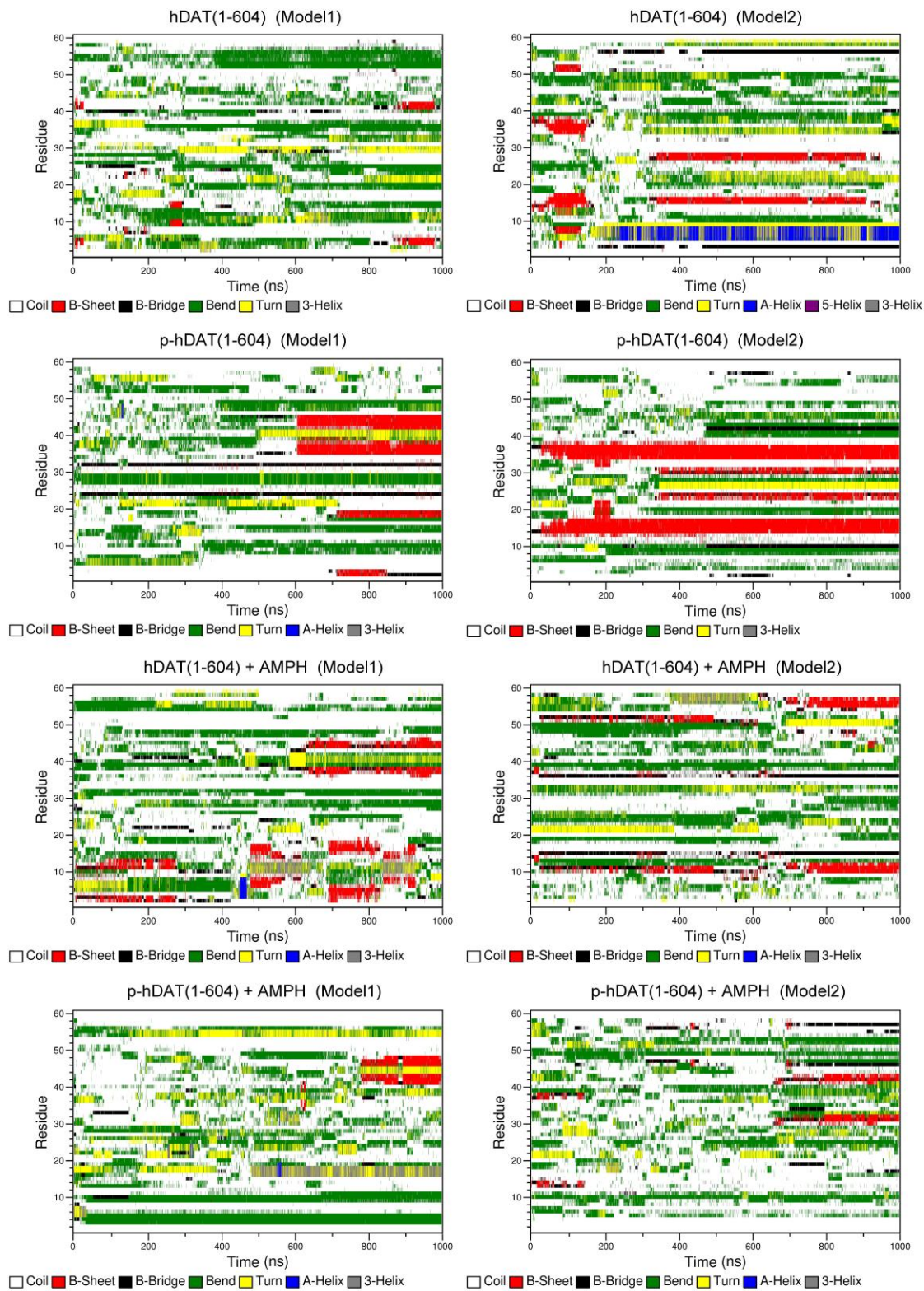| Residue in N-terminal	Residue in IC	Frequency	Assignment	Residue in N-terminal	Residue in IC	Frequency	Assignment
Gln58	Asp59	1.00	N-terminal	Arg51	Phe338	0.74	IL3
Ala57	Asp59	0.87	N-terminal	Ser53	Phe338	0.63	IL3
Ala57	Arg60	0.95	N-terminal	Met1	Asp436	1.00	TM8
Gln58	Arg60	0.70	N-terminal	Ser2	His442	0.92	IL4
Ser2	Arg60	0.54	N-terminal	Arg51	Tyr499	0.93	IL5
Arg51	Phe123	0.77	IL1	Asn49	Tyr499	0.58	IL5
Met1	Arg125	1.00	IL1	Arg51	Asp507	0.98	IL5
Glu56	Arg125	0.89	IL1	Arg51	Met511	0.82	IL5
Met1	Glu126	0.99	IL1	Thr43	Asp600	0.76	C-termimal
Met1	Ser334	0.99	IL3	Ser44	Asp600	0.67	C-termimal
Glu56	Tyr335	0.99	IL3	Lys5	Leu603	0.96	C-termimal
Ser2	Tyr335	0.99	IL3	Lys3	Leu603	0.90	C-termimal
Ala57	Tyr335	0.87	IL3	Val8	Leu603	0.90	C-termimal
Met1	Tyr335	0.84	IL3	Leu10	Leu603	0.62	C-termimal
Glu56	Lys337	0.85	IL3	Lys5	Val604	0.99	C-termimal

Table S6. The contact frequency between the N-terminal region and the intracellular region of AMPH-bound p-hDAT(1–604) (Model1, OF). IC indicates intracellular side. The electrostatic interactions are highlighted in red.

Residue in N-terminal	Residue in IC	Frequency	Assignment	Residue in N-terminal	Residue in IC	Frequency	Assignment
Gln58	Asp59	1.00	N-terminal	Val55	Lys260	0.56	IL2
p-Ser7	Arg60	1.00	N-terminal	Arg51	Thr261	0.72	IL2
p-Ser2	Arg60	1.00	N-terminal	Pro54	Gly263	0.71	IL2
Met1	Arg60	0.94	N-terminal	Ser53	Gly263	0.64	IL2
Leu10	Arg60	0.89	N-terminal	Pro54	Lys264	0.75	TM5
Gln58	Glu61	0.84	N-terminal	Pro54	Trp267	0.58	TM5
Leu10	Glu61	0.52	N-terminal	Val55	Phe332	0.97	IL3
Met11	Glu61	0.50	N-terminal	Glu56	Tyr335	0.94	IL3
Gln52	Trp63	0.86	N-terminal	Val55	Tyr335	0.85	IL3
Gln58	Trp63	0.78	N-terminal	Ala57	Asn336	0.88	IL3
Ser53	Trp63	0.75	N-terminal	Ala57	Lys337	0.91	IL3
Pro54	Trp63	0.71	N-terminal	Gln58	Lys337	0.51	IL3
Glu56	Trp63	0.56	N-terminal	Lys3	Phe338	0.92	IL3
Ala57	Trp63	0.52	N-terminal	Pro17	Thr432	0.50	TM8
Pro54	Asp68	0.56	TM1a	Pro17	Ile435	0.58	TM8
Val55	Phe69	0.97	TM1a	Pro21	His442	0.50	IL4
Pro54	Phe69	0.63	TM1a	Lys5	Glu602	0.97	C-termimal
Val55	Ser72	0.82	TM1a	p-Ser4	Glu602	0.92	C-termimal
Pro54	Ser72	0.57	TM1a	Lys3	Leu603	0.89	C-termimal
Val55	Val73	0.77	TM1a	p-Ser4	Leu603	0.84	C-termimal
Val55	Phe76	0.52	TM1a	p-Ser4	Val604	0.83	C-termimal
Lys3	Arg125	0.74	IL1	Lys3	Val604	0.76	C-termimal
Ser53	Lys260	0.98	IL2	Lys5	Val604	0.61	C-termimal
Glu56	Lys260	0.79	IL2				

Note: A contact occurs if any atom in the N-terminal region is within 3 Å of any atom in the TM domains, and only a contact frequency >0.50 (50%) is shown.

Fig. S27. Secondary structures calculated for the N-terminal in different systems. The formation of stable β-strands in p-hDAT(1–604) (Model2) was observed.

Table S7. The contact frequency between the N-terminal region and the intracellular region in the full-length p-hDAT+AMPH (Model1, OF). IC indicates intracellular side and IL indicates intracellular loop. The electrostatic interactions are highlighted in red.

| Residue in N-terminal	Residue in IC	Frequency	Assignment	Residue in N-terminal	Residue in IC	Frequency	Assignment
Gln58	Asp59	1.00	N-terminal	Pro54	Trp267	0.53	TM5
Lys3	Asp59	1.00	N-terminal	Pro17	Tyr335	1.00	IL3
Val15	Asp59	0.89	N-terminal	Gln58	Lys337	0.98	IL3
p-Ser2	Arg60	1.00	N-terminal	Ala57	Lys337	0.76	IL3
p-Ser12	Arg60	0.89	N-terminal	Lys3	Phe338	0.93	IL3
Gln58	Arg60	0.54	N-terminal	Pro21	Ile435	0.61	TM8
Gln58	Glu61	1.00	N-terminal	Asn22	His442	0.78	IL4
Gln52	Trp63	1.00	N-terminal	Lys5	Glu602	1.00	C-terminal
Ala57	Trp63	0.99	N-terminal	p-Ser4	Glu602	0.98	C-terminal
Pro54	Trp63	0.86	N-terminal	p-Ser4	Leu603	0.99	C-terminal
Ala57	Gly64	0.95	N-terminal	Lys3	Leu603	0.97	C-terminal
Pro54	Gly64	0.91	N-terminal	Lys3	Val604	0.85	C-terminal
Val55	Phe69	0.95	TM1a	p-Ser4	Val604	0.72	C-terminal
Pro54	Phe69	0.59	TMa1	Met1	Arg606	0.94	C-terminal
Val55	Ser72	0.56	TM1a	p-Ser4	Arg606	0.76	C-terminal
Pro54	Ser72	0.54	TM1a	Lys3	Arg606	0.56	C-terminal
p-Ser4	Arg125	1.00	IL1	Lys5	Arg606	0.50	C-terminal
Ala16	Arg125	0.93	IL1	Met1	Val609	0.79	C-terminal
Lys5	Arg125	0.88	IL1	p-Ser2	Val609	0.75	C-terminal
Lys3	Arg125	0.88	IL1	p-Ser7	Arg610	1.00	C-terminal
Ser53	Lys260	1.00	IL2	Met1	Arg610	0.86	C-terminal
Val55	Lys260	0.88	IL2	p-Ser2	Gln611	0.71	C-terminal
Glu56	Lys260	0.70	IL2	p-Ser7	Thr613	1.00	C-terminal
Pro17	Lys260	0.60	IL2	p-Ser12	Arg615	1.00	C-terminal
Glu56	Thr261	0.99	IL2	Gly9	Arg615	1.00	C-terminal
Ser53	Thr261	0.93	IL2	Val8	Arg615	1.00	C-terminal
Arg51	Thr261	0.73	IL2	Leu10	Arg615	0.97	C-terminal
Ser53	Gly263	0.97	IL2	p-Ser7	Arg615	0.96	C-terminal
Pro54	Gly263	0.52	IL2	Leu10	His616	0.67	C-terminal
Pro54	Lys264	0.88	TM5	Leu10	Trp617	0.90	C-terminal
Ser53	Lys264	0.74	TM5	Met11	Trp617	0.87	C-terminal
Gln52	Lys264	0.64	TM5	Val40	Trp617	0.51	C-terminal

Table S8. The contact frequency between the N-terminal region and the intracellular region in the full-length hDAT (Model2, IF). IC indicates intracellular side and IL indicates intracellular loop. The electrostatic interactions are highlighted in red.

Residue in N-terminal	Residue in IC	Frequency	Assignment	Residue in N-terminal	Residue in IC	Frequency	Assignment
Gln58	Asp59	1.00	N-terminal	Gly39	Gln503	0.54	IL5
Met1	Asp59	0.82	N-terminal	Gln41	Gln503	0.51	IL5
Leu31	Phe123	0.65	IL1	Lys35	Asp506	0.68	IL5
Met1	Arg125	0.97	IL1	Leu31	Gln510	0.99	IL5
Glu56	Arg125	0.88	IL1	Ile32	Gln510	0.99	IL5
Ser2	Arg125	0.55	IL1	Val34	Gln510	0.94	IL5
Ser2	Glu126	0.79	IL1	Lys35	Gln510	0.91	IL5
Met1	Glu126	0.52	IL1	Leu31	Met511	0.94	IL5
Gln41	Ile134	0.97	IL1	Ile32	Gly513	0.84	IL5
Leu42	Ile134	0.91	IL1	Leu42	Ile595	0.93	C-terminal
Met1	Ser334	0.60	IL3	Val40	Pro597	0.74	C-terminal
Leu31	Phe338	0.94	IL3	Gln41	Pro597	0.69	C-terminal
Glu30	Phe338	0.68	IL3	Ser2	Arg601	0.52	C-terminal
Glu30	Thr339	0.75	IL3	Lys3	Arg601	0.51	C-terminal
Ile32	Thr339	0.50	IL3	Val8	Arg601	0.51	C-terminal
Val15	Gln439	0.67	IL4	Val8	Leu603	0.93	C-terminal
Val15	Hsd442	0.59	IL4	Pro50	Val604	0.56	C-terminal
Val15	Arg443	0.77	IL4	Leu47	Arg606	0.58	C-terminal
Pro17	Arg443	0.64	IL4	Leu10	Trp617	0.54	C-terminal
Leu42	Phe498	0.96	IL5	Met11	Trp617	0.50	C-terminal
Gln41	Phe498	0.61	IL5	Leu10	Leu618	0.95	C-terminal
Gln41	Tyr499	0.92	IL5				

Table S9. The contact frequency between the N-terminal region and the intracellular region in the designed full-length hDAT (OF). IC indicates intracellular side and IL indicates intracellular loop. The electrostatic interactions are highlighted in red.

| Residue in N-terminal	Residue in IC	Frequency	Assignment	Residue in N-terminal	Residue in IC	Frequency	Assignment
Gln58	Asp59	1.00	N-terminal	Met1	Tyr335	0.53	IL3
Ala57	Asp59	0.59	N-terminal	Glu56	Lys337	0.61	IL3
Gln58	Arg60	0.57	N-terminal	Ser53	Phe338	0.56	IL3
Glu56	Arg125	0.76	IL1	Met1	Asp436	0.68	TM8
Met1	Arg125	0.64	IL1	Arg51	Gln510	0.5	IL5
Met1	Glu126	0.77	IL1	Arg51	Met511	0.52	IL5
Met1	Ser334	0.62	IL3	Lys3	Asp600	0.62	C-terminal
Glu56	Tyr335	0.56	IL3	Lys5	Glu602	0.65	C-terminal
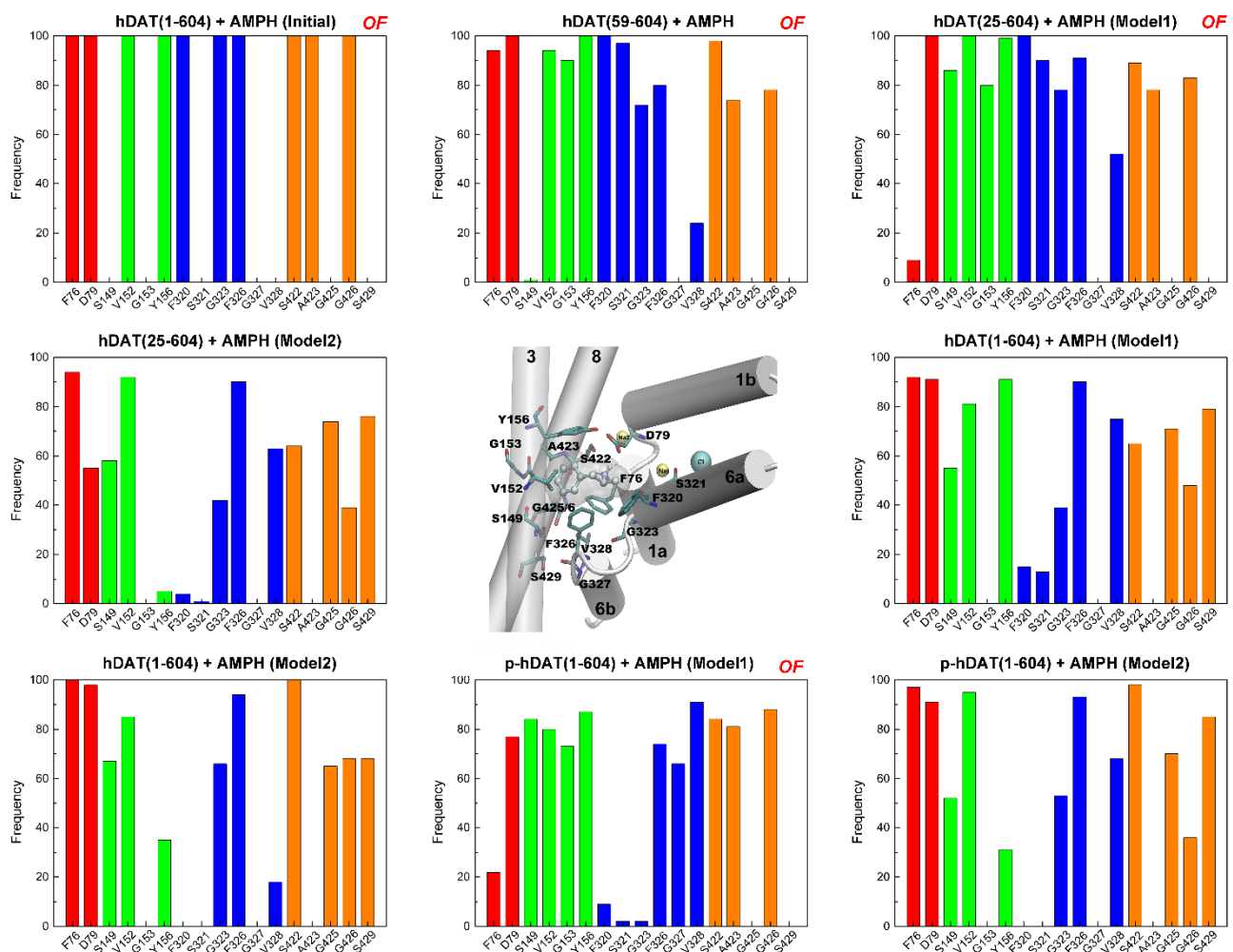
Fig. S28. Residues interacting with AMPH and their contact frequencies (%) calculated for all AMPH-bound systems. Contact frequency for residues in TM1 (Phe76 and Asp79), TM3 (Ser149, Val152, Gly153, and Tyr156), TM6 (Phe320, Ser321, Gly323, Phe326, Gly327, and Val328), and TM8 (Ser422, Ala423, Gly425, Gly426, and Ser429) are colored in red, green, blue, and orange, respectively. The binding pocket of AMPH is shown in the center. One Na$^+$ (Na1) is coordinated with Ser321, and the other Na$^+$ (Na2) is coordinated with Ser422. hDAT in the outward-facing open conformation is denoted as OF, and the remaining hDATs are in the inward-facing open conformations. A contact occurs if any atom in AMPH is within 3 Å of any atom in hDAT.
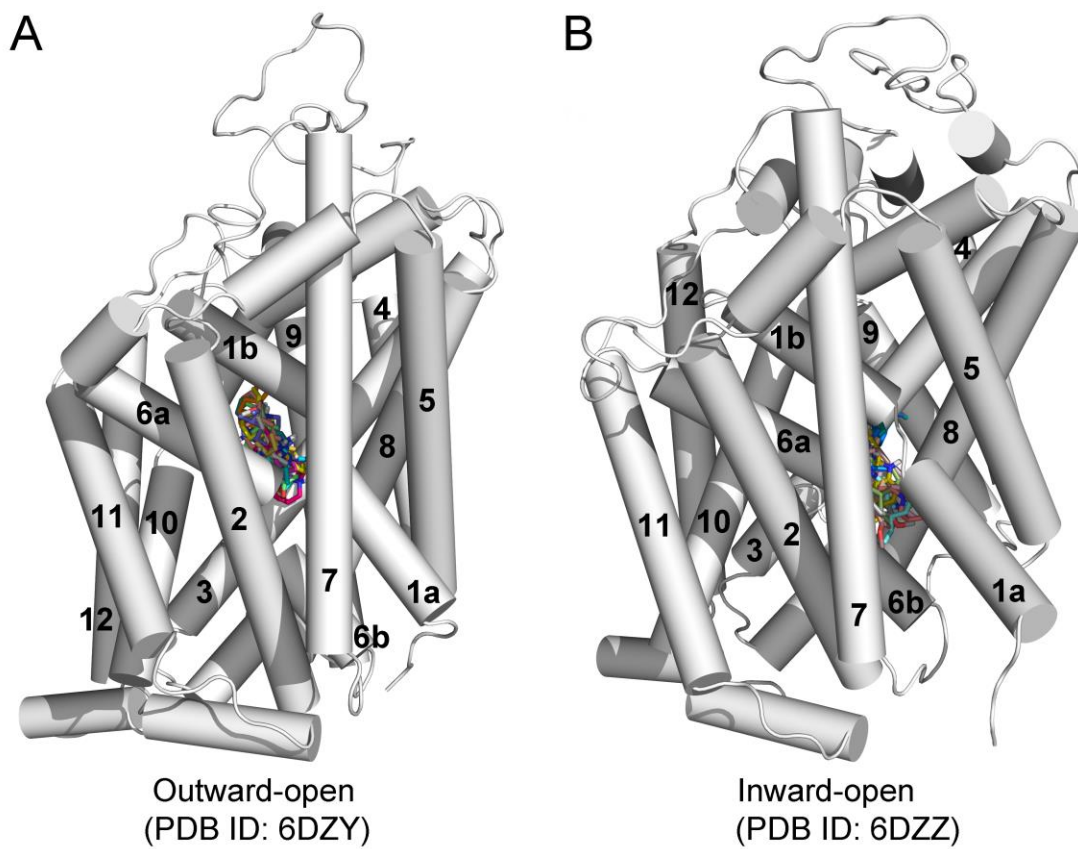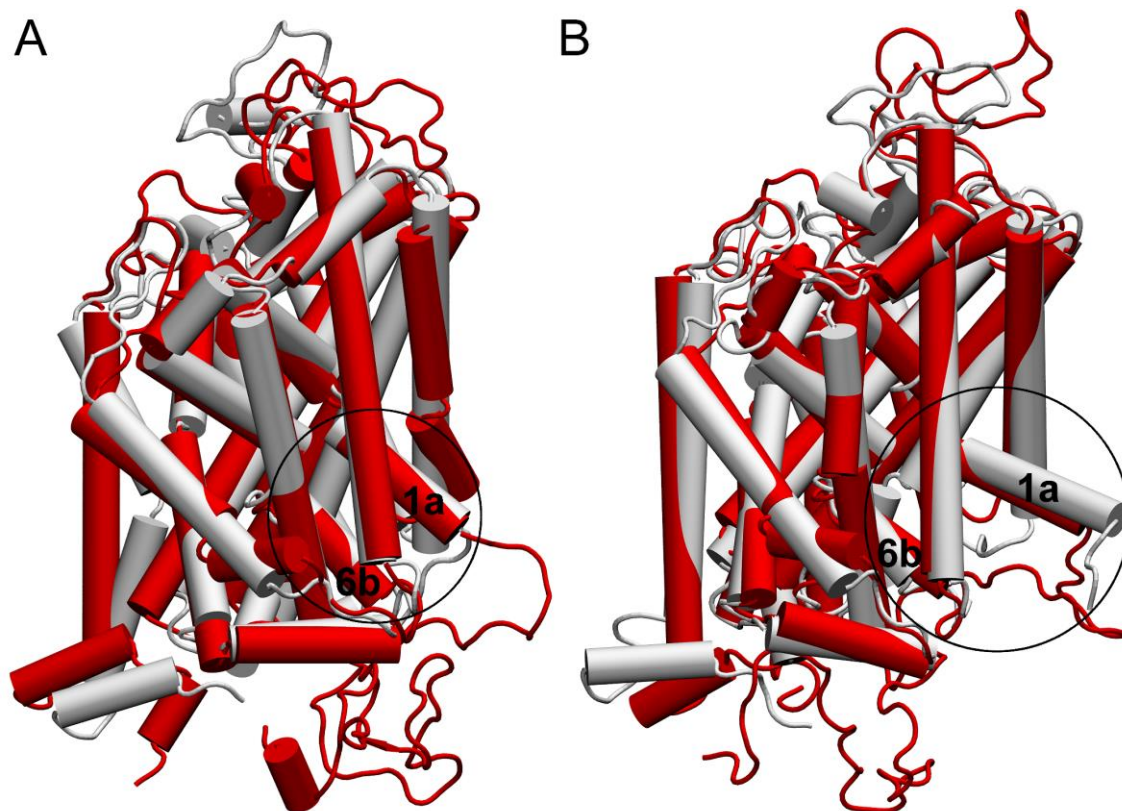
Fig. S29. Molecular docking of ibogaine to hSERT in the outward-open and inward-open conformations.
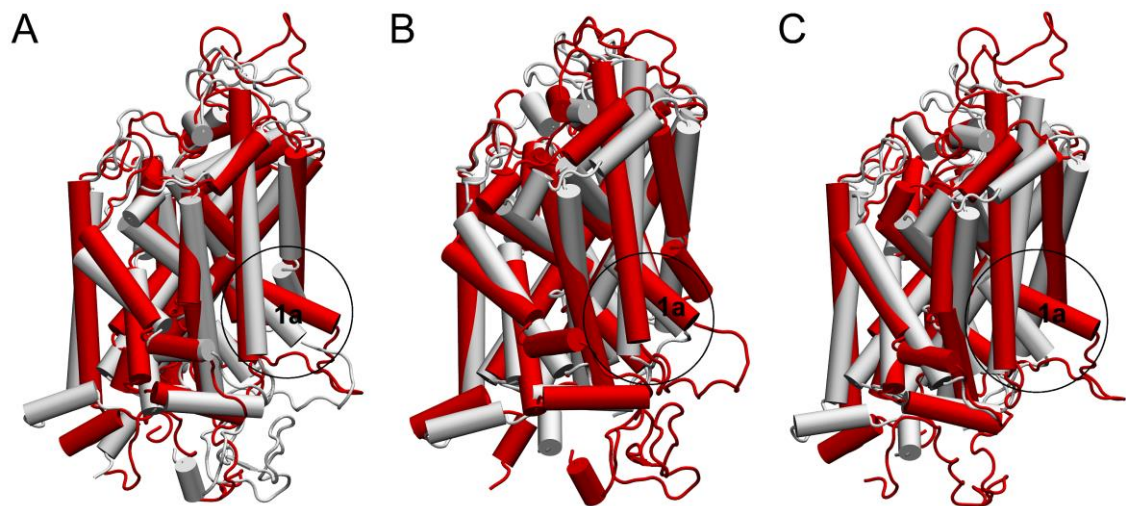
Fig. S30. Representative conformations of hDAT obtained from MD simulations. (A) Superposition of the outward-open (white) and the inward-open (red) conformations. (B) Superposition of the crystal structure of dDAT (in the outward-open conformation, PDB ID: 4XP9, white) and the outward-open (red) conformation of hDAT obtained from the present MD simulations. (C) Superposition of the crystal structure of dDAT (in the outward-open conformation, PDB ID: 4XP9, white) and the inward-open (red) conformation of hDAT obtained from the present MD simulations. The movement of transmembrane helix 1a was highlighted in circle.

Fig. S31. Superposition of representative conformations of hDAT obtained from MD simulations and the conformations of hSERT. (A) Superposition of the outward-open (white) conformation of hSERT (PDB ID: 6DZY) and the outward-open (red) conformation of hDAT. (B) Superposition of the inward-open (white) conformation of hSERT (PDB ID: 6DZZ) and the inward-open (red) conformation of hDAT. The positions of transmembrane helix 1a and 6b were highlighted in circle.

References

1   Laskowski, R. A. & Swindells, M. B. LigPlot+: Multiple Ligand−Protein Interaction Diagrams for Drug Discovery. *Journal of Chemical Information and Modeling* **51**, 2778-2786, doi:10.1021/ci200227u (2011).

2   Wang, J., Cieplak, P. & Kollman, P. A. How well does a restrained electrostatic potential (RESP) model perform in calculating conformational energies of organic and biological molecules? *Journal of Computational Chemistry* **21**, 1049-1074, doi:10.1002/1096-987x(200009)21:12<1049::aid-jcc3>3.0.co;2-f (2000).

3   Frisch, M. J.; Trucks, G. W.; Schlegel, H. B.; Scuseria, G. E.; Robb, M. A.; Cheeseman, J. R.; Zakrzewski, V. G.; Montgomery, J. A., Jr.; Stratmann, R. E.; Burant, J. C.; Dapprich, S.; Millam, J. M.; Daniels, A. D.; Kudin, K. N.; Strain, M. C.; Farkas, O.; Tomasi, J.; Barone, V.; Cossi, M.; Cammi, R.; Mennucci, B.; Pomelli, C.; Adamo, C.; Clifford, S.; Ochterski, J.; Petersson, G. A.; Ayala, P. Y.; Cui, Q.; Morokuma, K.; Malick, D. K.; Rabuck, A. D.; Raghavachari, K.; Foresman, J. B.; Cioslowski, J.; Ortiz, J. V.; Stefanov, B. B.; Liu, G.; Liashenko, A.; Piskorz, P.; Komaromi, I.; Gomperts, R.; Martin, R. L.; Fox, D. J.; Keith, T.; Al-Laham, M. A.; Peng, C. Y.; Nanayakkara, A.;

Gonzalez, C.; Challacombe, M.; Gill, P. M. W.; Johnson, B.; Chen, W.; Wong, M. W.; Gonzalez, C.; Pople, J. A. Gaussian 03, Revision E.01; Gaussian Inc.: Wallingford CT, 2004.